NASW-4435

IN-05-CR

73939

p 73

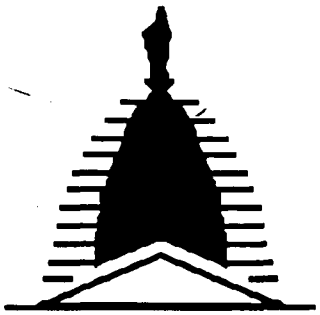

UNIVERSITY of
NOTRE DAME

NASA/USRA UNIVERSITY ADVANCED DESIGN PROGRAM 1990-1991

UNIVERSITY SPONSOR
BOEING COMMERCIAL AIRPLANE COMPANY

FINAL DESIGN PROPOSAL

DELTA GROUP - NOOD RIDER 821

A Proposal in Response to a Commercial Air Transportation Study

May 1991

Department of Aerospace and Mechanical Engineering
University of Notre Dame
Notre Dame, IN 46556

(NASA-CR-190020) FINAL DESIGN PROPOSAL: DELTA GROUP-NOOD RIDER 821(TM) (Notre Dame Univ.) 73 p

N92-21374

CSCL 01C

Unclas

G3/05 0073939

The Nood Rider 821™ Design Document

Second Edition

C. B. Pastega
Group Leader

B. P. Vahey
Chief Engineer
Aerodynamics Group

K. W. Hoffman
Propulsion Group and
Motivation Expert

M. C. Doherty
Performance Specialist

M. J. Fay
Weights and Structures Group

A. L. Konesky
Propulsion Group

D. C. Lilly
Weights and Structures Group

D. J. Moody
Controls and Stability Group

Delta Group, Inc.
Notre Dame, Indiana

This document was set in New Century Schoolbook
The editors were A. Konesky, K. Hoffman, C. Pastega, and B. Vahey
All material written and edited on Macintosh Computers
using Microsoft Word 4.0.

The Nood Rider™ Design Document

This document was created for the sole purpose of fulfilling the course requirements for the University of Notre Dame's senior Aerospace Design Class, AE 441. Credit is due to *most* of the Aerospace faculty for their instruction and guidance, and especially to the course teaching assistants Mr. David Carey and Mr. Kevin Costello for their insight.

TABLE OF CONTENTS

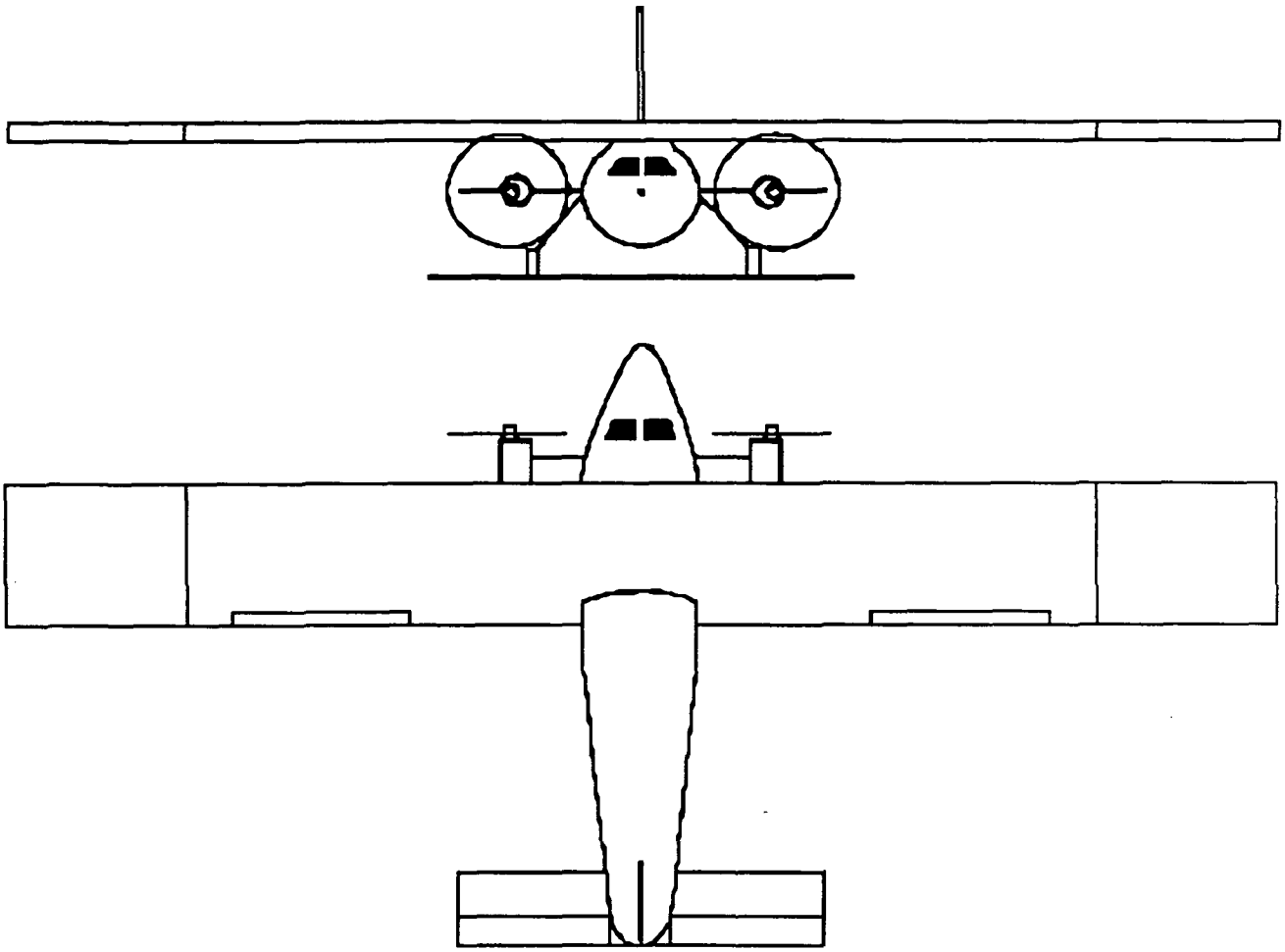

NOOD RIDER 821

Scale 32:1

Nood Rider 821™ Specifications

Parameter	Value	Symbol
Cruise Reynolds Number	155,000	Re
Cruise Velocity	10 m/s	V_{cruise}
Engine Type	Astro 05	--
Engine Max Power @ RPM	134.3 Watts @ 17,450 RPM	P_{max}
Propellers	8 X 4	--
Endurance	265 sec	E_{max}
Range	2470 m	R_{max}
Max Rate of Climb	6.02 m/s	R/C_{max}
Takeoff Distance	13.3 m	S_{to}
Landing Distance	20 m	S_{land}
Fuselage Max Diameter	19.1 cm	D_{max}
Fuselage Length	107.7 cm	L_{fuse}
Wing Surface Area	.542 m^2	S_w
Wing Root Chord	25.4 cm	c
Wing Taper Ratio	1	τ
Wing Span	2.13 m	b
Wing Aspect Ratio	8.40	AR_w
Wing Max Coef. of Lift	1.14	$C_{L,max}$
Wing Dihedral	0°	Γ
Wing Incidence Angle	3.75°	i_w
Vertical Tail Area	0.052 m^2	S_v
Horizontal Tail Area	0.039 m^2	S_h

1. EXECUTIVE SUMMARY

The Nood Rider 821™, designed and manufactured by the Delta Group, is one of the best answers to the travel demands of Aeroworld. Our aircraft provides a fast, efficient, and relatively inexpensive alternate mode of transportation to the people of Aeroworld. In addition, the Nood Rider 821™ is able to expand with the growing needs of the market.

The Nood Rider 821™ offers safety far superior to that of our competitors. A number of the routes the aircraft will be used on will be over large bodies of water. With its twin engine configuration, the aircraft can remain safely airborne while diverting to the nearest airport. Although the aircraft cannot takeoff with one engine out, it can be brought to a stop safely with adequate control.

The Delta Group also offers the greatest amount of time savings. The Nood Rider 821™ cruises at a velocity greater than or equal to that of our competitors. At a cruise velocity of 10 m/s, the Nood Rider 821™ will be able to move passengers to their destinations with a large time savings. Since the passenger is paying a premium for air transportation, we felt it important to maximize this time savings. With the absence of a drag penalty for flying at mach numbers close to one, there is no disadvantage with flying at this velocity.

The passenger payload of 50 and the foldable wingspan of the Nood Rider 821™ gives a greater flexibility in our departure schedule. The on-ground wingspan of 1.52 m allows the Nood Rider 821™ to utilize all of the gates available in Aeroworld. The relatively small passenger payload allows for multiple daily departures from every city in Aeroworld. Flexibility in planning an itinerary is paramount in every travellers needs, and the Nood Rider 821™ is able to satisfy them.

Maintaining the aircraft was always an important consideration when designing the aircraft. The engines, mounted on pylons extending from the fuselage, are easily accessible. This allows for ease of routine maintenance or replacement of the engine if necessary. The structure of the entire aircraft is of the simplest design. The wing is a three spar structure with ribs and stringers. The empennage is a two spar configuration of similar construction. The fuselage consists of circular bulkheads with longerons running between. All of this allows for easy maintenance and repair should the aircraft be subjected to any damage.

With a cruise range of 1233 m, the Nood Rider 821™ is able to remain competitive with the other modes of transportation in Aeroworld. The total selling price of the Nood Rider 821™ is $368,000. The per flight operating cost of the aircraft is $70,843. Charging the passenger a ticket price of $12 per 50 feet (15.24 m) plus a flat fee of $100, allows the operator to recoup all of the operating costs, which include depreciation for yearly replacement of the aircraft, even when flying at a passenger load factor of 0.70. This makes the Nood Rider a viable alternative to trains, which charge a price of $6.25 per 50 feet plus a flat fee of $50, or boats, which charge a price of $8.00 per 50 feet plus a flat fee of $65.

Therefore, we will be basing the success of our aircraft on several important figures of merit. To wit, the mass of the aircraft, the cruise range, and the operating cost per aircraft. Taking all of these factors into consideration, the Delta Group believes that the Nood Rider 821™ will prove to be a safe, fast, efficient, and viable alternative mode of transportation.

2. PRELIMINARY CONCEPT

The Nood Rider 821™ is the concept which the Delta Group feels best fulfills the travel needs of Aeroworld. Many different concepts were considered in order to meet these needs. Through a process of design, the group arrived at the preliminary design as presented in this document. Although the design is not 100% complete, all of the preliminary engineering has been completed, and the final design should not deviate greatly from the design proposed here.

2.1 Review of Design Requirements

The design for the Nood Rider 821™ was based on the proposal for design submitted to the Delta Group. The following is from the *Request for Proposals* given to the group.

> **Problem Statement**
> The project goal will be to design a commercial transport which will provide the greatest potential return on investment in a new airplane market, Aeroworld (Figure 1.1). Maximizing the profit that your airplane design will make for your customer, the airline, will be the design goal. You may choose to design the plane for any market in the fictitious world from which you believe the airline will be able to realize the most profit. This will be done by careful consideration and balancing of the variables such as the number of "passengers" carried, range/payload, fuel efficiency, production costs, and maintenance and operation costs. Appropriate data for each is included in the project description.
>
> The "world" market in which the airline will operate is shown in Figure 1.1. The number of people who wish to travel between each possible pair of cities each day is provided. Other useful information is given regarding each city: details on location, runway length and number of gates available to your airline and their size. The up-start airline may operate in any number of markets provided that they use only one airplane design and its derivatives (your company does not have the engineering manpower to develop two different designs for them). Consider derivative aircraft as a possible cost-effective way of expanding its markets.

Based on this proposal, the Delta Group began to study the travel demands of Aeroworld. By doing this, the group was able to establish the mission of our aircraft and a number of design objectives.

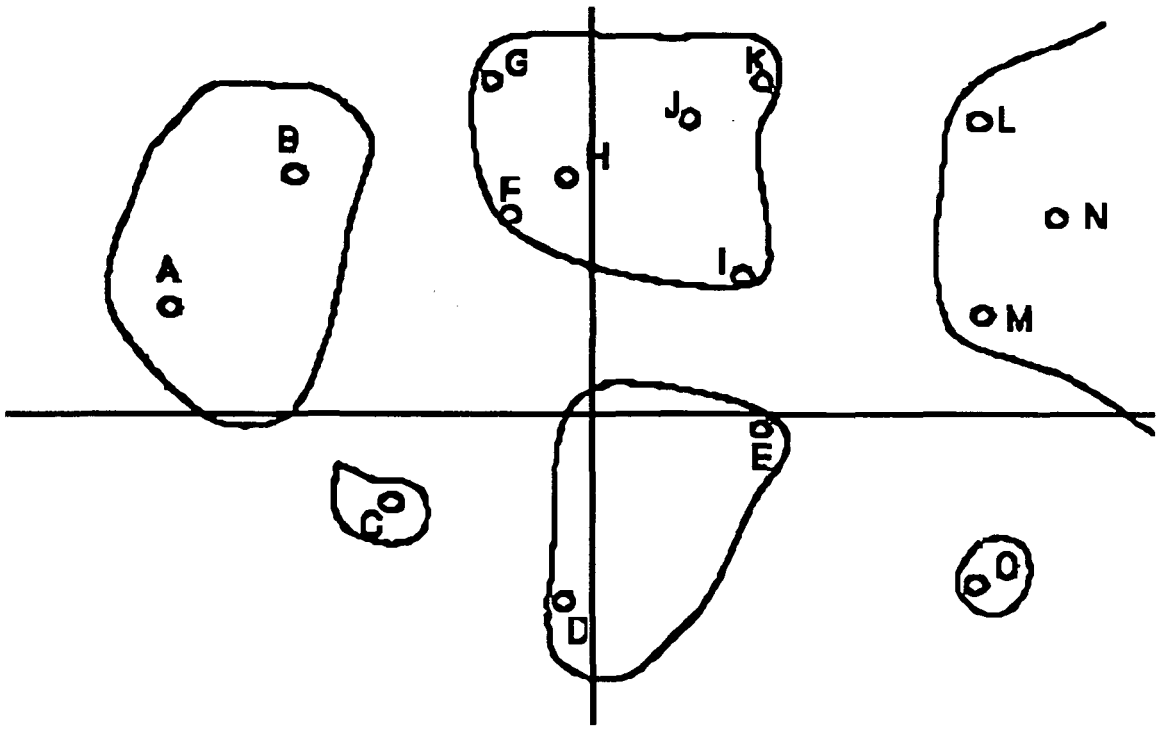

AEROWORLD

Figure 2.1

2.2 Mission Definition and Design Objectives

The Delta Group decided that our main goals were to serve all of the cities in Aeroworld in the fastest, most efficient manner. We wanted to be able to transport all of the passengers wishing to travel between the most popular cities, as well as to fly between the less popular cities. In doing this we wanted to fly the majority of flights with a near 100% passenger load factor.

It seemed unreasonable to establish the range of our aircraft based on the longest route, and it seemed just as unreasonable to determine our passenger payload based on the smallest passenger loads. To combat these differences, the group decided to establish a hub system in Aeroworld. By establishing hubs at cities A, F, J, and N, all cities in Aeroworld could be serviced with the longest flight being 1233 m. Our total aircraft range could then be set at 1828 m. The total range includes the 1233 m cruise range, loiter time, and diversion to the nearest airport.

With the range established, the passenger payload had to be determined. One of the purposes in choosing air travel, by our estimation, is convenience. The passenger should have a wide variety of choices when deciding a flight time. It was our desire to meet all inter-hub travel demands with 10 flights per day, and all outlying city demands with 4 flights per day. This would allow the passenger some flexibility in choosing a travel time. Keeping this number of flights in mind, we determined that all of the needs of Aeroworld could be serviced with a 50 passenger aircraft. This would allow for a variety of flights each day and passenger loads near capacity on all flights.

The Delta Group also felt that one of the purposes of choosing air travel is time savings. Our aircraft should be able to move passengers to their destinations as quickly as possible. With this in mind, the group set a goal of 10 m/s for our cruise velocity.

A number of other objectives were set at this early stage in the concept proposal. They were as follows.

1. Twin engines due to overwater routes.
2. 3-axis control (Ailerons, elevator, and rudder).
3. Takeoff and Landing Distance no greater than 15 meters.
4. Turning radius no larger than 18 meters.
5. A maximum flight altitude of 7.62 meters.

These objectives and design goals allow for all of the constraints and demands of Aeroworld to be satisfied in a safe and efficient manner.

2.3 Concept Selection Studies

The preliminary concept as envisioned for the Nood Rider 821™ was determined through a process of review of different concepts proposed by each of the eight members of the Delta Group. Concepts were accepted or rejected based on their compliance with the overall group objectives and design goals. In addition, the concepts were scrutinized based on safety, cost, ease of construction, ease of maintenance, and engineering merit. (Engineering merit meaning how much sense the concept makes from an engineer's standpoint.)

Eight concepts were submitted for the group's approval. The concepts varied on nearly every possible aspect. There were high wing and low wing concepts, twin

engine and single engine concepts, high tail and low tail concepts, etc. After careful review, none of the concepts were accepted. However, the best aspects from each concept were taken and the Nood Rider 821™ was conceived. Each of the key features of the Nood Rider 821™ are listed below with a brief summary of the rationale that lead to the choosing of each.

Round Fuselage. The Delta Group chose the round fuselage from a passenger comfort point of view. In the "real-world" version of the Nood Rider 821™, a pressurized cabin would allow for the aircraft to fly above the clouds, thus giving a smoother flight and more comfortable environment to the passenger. A round fuselage allows for the cabin to be pressurized.

Tail Dragger. In the absence of high lift devices, the group saw a need to generate an increased coefficient of lift at takeoff. The tail dragger configuration naturally sets the main wing at an angle of attack. By keeping a down load on the tail, the wing will remain at an angle of attack for the duration of the ground roll. When the ground speed reaches a sufficient value, the airplane can then be flown off of the ground without any need for rotation.

Flat Plate Tail. The main reason for choosing the flat plate tail was its ease of construction. The only other real choice was to build a symmetric tail. The benefit of a symmetric tail is that it cuts down on drag. However, our flat plate tail contributes minimally in the overall drag analysis. Therefore, there is no real benefit in using a symmetric tail, and the flat plate tail provides the benefit of ease of construction.

High Wing. The Delta Group chose a high wing configuration with ailerons and without dihedral. The high wing exhibits superior roll stability over the low wing configuration. This allows for the simpler construction of a no dihedral wing. The addition of ailerons allows for banked, coordinated turns which will be more easily adapted to the confines of Aeroworld.

Foldable Wingspan. The concept as envisioned will employ a wingspan of 2.13 m in order to meet the lift requirements of the Nood Rider 821™. The group felt a need for a greater number of gates than those which can be utilized at the airports of Aeroworld using a 2.13 m wingspan. By folding the outer 30.5 cm portion of the

wing upon landing, the Nood Rider 821™ will be able to utilize all of the gates in Aeroworld.

Twin, Pylon Mounted Motors. The main factor in choosing the twin engine configuration was safety. We felt the overwater routes dictated the need for the aircraft to remain airborne with one engine out. The pylon mounting arose from the desire to create a "clean" wing. By placing the engines on pylons which attach to the fuselage, the structural and aerodynamic complications which would be created by mounting the engines in the wings are eliminated. The pylon mounting also allows for easier maintenance and replacement, if necessary, of the engines. This would be a benefit to possible customers.

The above are the key features of the Nood Rider 821™ as envisioned in its preliminary concept. These features also lend themselves to making derivative versions possible. Derivative versions would allow the Nood Rider 821™ to accommodate the growing demands of Aeroworld. Some of the derivative models possible include: adding a fuselage plug aft of the wing to allow for a passenger payload of up to 75, extending the range by increasing the amount of fuel carried, and a freighter version to meet the shipping demands of Aeroworld. All of these are possible due to the power available from the twin engine configuration and the extra lifting ability of the main wing. At present, none of these possibilities have been explored in depth; however, the current configuration will allow a slightly increased gross weight.

3. PERFORMANCE

3.1 Range and Endurance

As with most studies in aircraft design, range and endurance are the most critical performance parameters. The longest distance between Aeroworld cities flown by the Nood Rider 821™ is 1233 m. The distance to an alternate airport is 628 m, and the distance necessitated by a sixty second loiter (at the cruise velocity of 10 m/s) is 600 m. With a maximum overall endurance of 2470 m, the Nood Rider 821™ is capable of efficiently executing its mission while meeting all prescribed requirements. The time to cruise is approximately 124 s. Additionally, the time to an alternate airport is 63 s and loiter time is 60 s, giving a total cruise endurance of 247 s. The design group estimates that five seconds of ground handling time must be added, along with a takeoff time of 3.5 s and a time to climb of 8.6 s; therefore, 265 s of battery power are required. The Nood Rider 821™ propulsion system is capable of providing all of the necessary power for operation.

FLIGHT VELOCITIES AND OTHER PERFORMANCE PARAMETERS:

Cruise Velocity	10 m/s (.94 M)
Stall Velocity	7.16 m/s
Takeoff Velocity	9.1 m/s
Maximum Velocity	14.8 m/s
Maximum Rate of Climb	1.87 m/s
Best Range Glide Angle (γ_{br})	-4.13°
Takeoff Distance	13.3 m
Landing Distance	20.0 m

The cruise velocity was set at 10 m/s in accordance with the design objectives. In calculating maximum range, maximum endurance, endurance at maximum range, and range at maximum endurance, we found that cruising at 10 m/s corresponded to the maximum propeller efficiency. Thus, for our configuration, our maximum range was the range that corresponded to the maximum endurance, and vice versa.

Stall velocity was calculated using Equation 3.1 taken from Anderson's Introduction to Flight.

$$V_{stall} = (2W/ \rho_{\infty} S C_{L,max})^{1/2} \qquad 3.1$$

The takeoff velocity was calculated as $1.2V_{stall}$. Maximum velocity was calculated from the maximum power available using Equation 3.2

$$V_{max} = \frac{J_{max}\, \eta_{max}}{d_{prop}} \qquad 3.2$$

where J_{max} is the maximum propeller advance ratio and η_{max} is the maximum propeller efficiency. The maximum rate of climb, R/C_{max} is limited by the aircraft stall angle, not the power available. Using Equation 3.3,

$$R/C_{max} = V_{max} \sin\Gamma_{stall} \qquad 3.3$$

we were able to arrive at the value stated in the chart above. The best range glide angle, $\gamma_{best\ range}$, was calculated using Equation 3.4 obtained from Hale's Introduction to Aircraft Performance, Selection, and Design,

$$\gamma_{best\ range} = -1 / E_m \qquad 3.4$$

where E_m is the maximum lift to drag ratio. The takeoff distance, d_{to}, was determined using Equation 3.5 found in Anderson's Introduction to Flight,

$$S_{T.O.} = \frac{1.44W^2}{g\rho_{\infty} S C_{L,max} \{T - [D + \mu_r(W - L)]_{0.7V_{T.O.}}\}} \qquad 3.5$$

where the thrust, T, was estimated from the relation: $T = C_t \rho n^2 (d_{prop})^4$, and μ_r, the coefficient of rolling friction, was estimated to be .05 for rubber on Astroturf. Similarly, the landing distance, S_L , was calculated using Equation 3.6 also taken from Anderson's Introduction to Flight.

$$S_L = \frac{1.69W^2}{g\rho_{\infty} S C_{L,max} [D + \mu_r(W - L)]_{0.7V_{T.O.}}} \qquad 3.6$$

For landing, a value of μ_r of .4 was used to take into account the effect of braking.

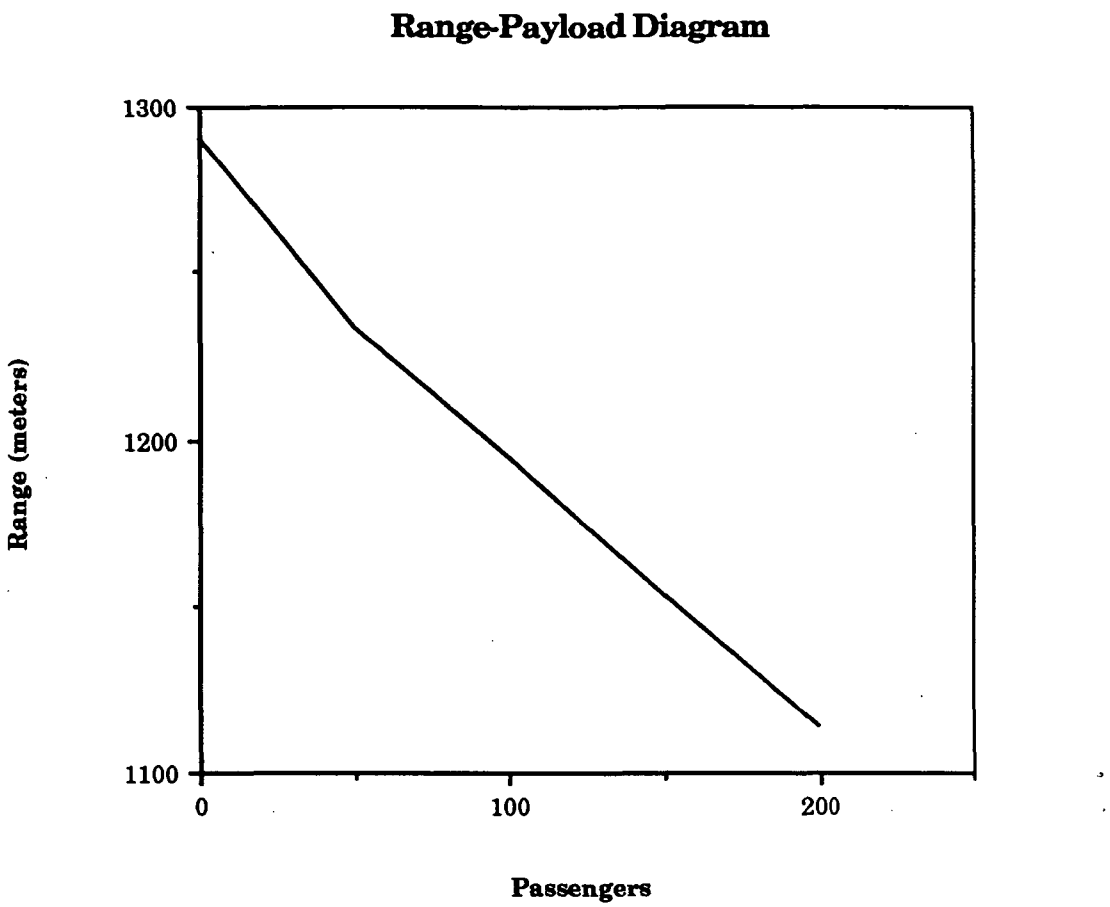

Figure 3.1

As can be seen in Figure 3.1, range is basically a linear function of payload, or in essence, of weight. This makes sense in that out of our 900 Mah battery a certain portion must be used for takeoff, alternate, and loiter, so whatever capacity could be used for cruise will diminish faster with greater weight.

4. AERODYNAMICS

The Nood Rider 821™ airplane's aerodynamic specifications can be broken down into four integral parts: airfoil selection, wing design, lifting characteristics, and drag prediction. The design process originally centered around the weight of the aircraft, which in turn affected the takeoff capabilities associated with the propulsion system. It was this weight estimate and takeoff distance which placed the original demands on the aerodynamic design. A wing was needed that would provide both adequate lift and performance at the desired cruise velocity and Reynold's number (155,000), without undue sacrifices in drag. Since the most important aspect of a wing's design is its airfoil section, this is where the aerodynamics study began.

4.1 Airfoil Selection

The airfoil selected for the Nood Rider 821™ was selected based on three design criterion--lift, drag, and geometry. It was necessary for the wing to have a strong lifting airfoil, that is one with both a high $C_{l_{max}}$ and a high lift curve slope. It was desired to have an airfoil with a flat drag bucket for values of C_l up to approximately 1.0, with low values of C_d relative to C_l. The wing geometry needed to be simple. This would allow more accurate duplication and also decrease the amount of construction time and cost. Using these three design criterion and Abbott and Doenhoff's Theory of Wing Sections, three airfoils were selected for closer study. They were: the NACA 4415, the NACA 23015, and the NACA 63-415. Each of these airfoils fulfilled the first two design criterion well, which separated them from the rest. Finally, the NACA 4415 was chosen as the design airfoil based on examinations of the three airfoil geometries and the fact that it also exhibited extremely strong lifting characteristics.. These geometries can be seen in Figure 4.1.

Airfoils Studied for the Nood Rider 821™

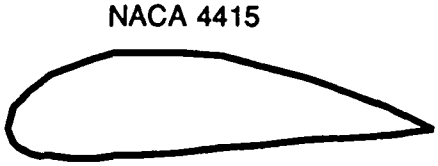

Figure 4.1

NACA 23015

NACA 63-415

Figure 4.1 (cont'd)

The NACA 4415 (Re = 155,000) has a $C_{l_{max}}$ of 1.42, a C_{l_α} of 5.58 rad^{-1} and an α_{stall} of approximately 15.0°. Its lift curve and drag polar can be seen in Figure 4.2[1]. These aerodynamic characteristics were as good as, if not better than, the other two airfoils. Also, as can be seen, its geometry is quite simple with no severe

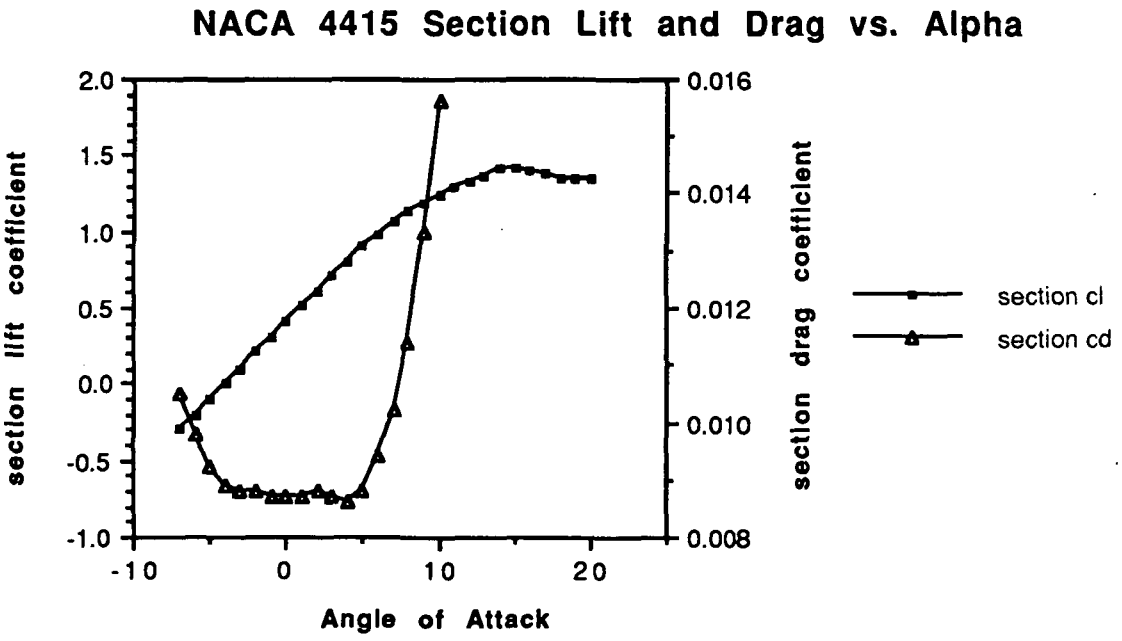

Figure 4.2

[1]Low Re Airfoils

deflections and a relatively flat bottom surface. This yields a significantly simpler construction than that of the other two airfoils. The next step in the aerodynamic design was to configure a wing that maximized the NACA 4415's assets.

4.2 Wing Design

The wing design for Nood Rider 821™ is the result of a study by the Delta Group which examined both efficiencies and L/D. From lift and drag considerations, it was desired to keep the wing efficiency above 0.97 and to fly at the highest value of L/D possible in order to maximize the range of the aircraft. There were several design constraints placed on the study--wingspan, cruise velocity, and wing surface area. The wingspan was limited to no greater than 2.13 m in order to fulfill the design objective to service the larger gates with the wing in the unfolded configuration. The cruise velocity was set at 10 m/s in order to satisfy the design goal to make flight time as short as possible. The surface area, S, was held constant at 0.542 m^2 in order to enable the aircraft to take off at all the airports. The remaining variables to be decided upon were taper ratio, τ, and aspect ratio, AR_w.

Using the computer program Linair 1.4 and varying the taper ratios from 0.5 to 1.0 and aspect ratios from 6 to 8.4 (the maximum obtainable), it was found that efficiency never fell below 0.98. Therefore, based on the design emphasis of keeping costs down, it appeared that using a taper ratio of 1.0 would not hamper the aircraft's aerodynamics and at the same time significantly reduce the amount of construction time involved with manufacturing the wing. From this point on in the study the efficiency was kept at 0.98 for consistency and only the aspect ratio was varied. Next, using the computer program Microsoft Excel, wing L/D ratios were calculated for the various AR_ws, as can be seen in Figure 4.3. As one can see, the aspect ratio of 8.4 gave the highest values of L/D. Therefore, 8.4 was selected as the optimum value and resulted in the Nood Rider 821™ having a wingspan of 2.13 m and a chord of 25.4 cm.

In order to fly at the maximum attainable L/D, the aircraft would have to break one of two design constraints--either decrease the speed by approximately 19% or decrease the wing surface area by 34%. Both of these possibilities were ruled unachievable. Another reason the maximum L/D design was deemed unfeasible

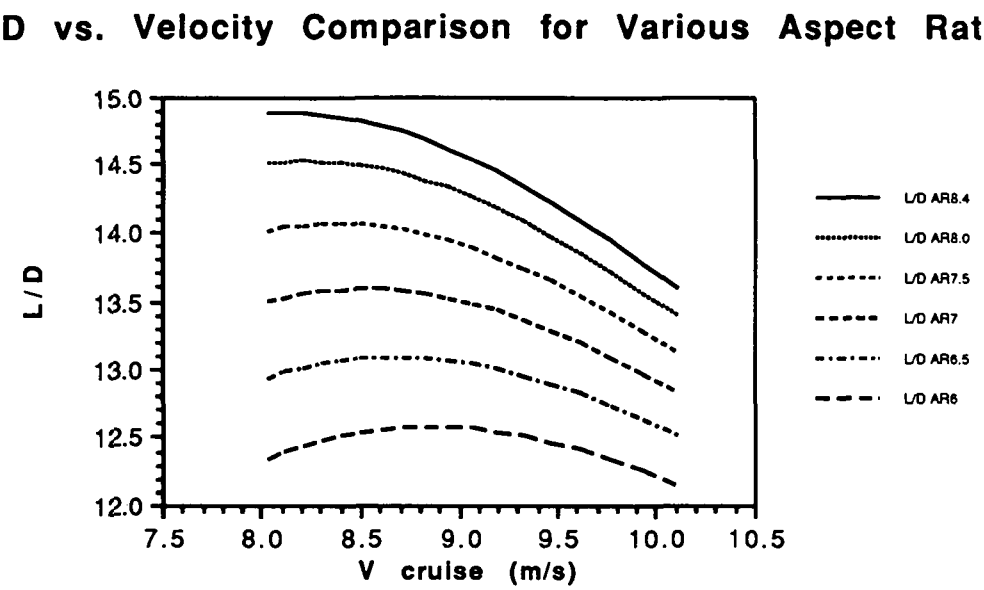

Figure 4.3

was because it required the wing to be mounted at an incidence angle of 6.6° for our desired cruise velocity with the decreased surface area. This would provide less than 3° of a climb angle before stall. This can be seen in Figure 4.4a. However, the design group desired at least 5°. Upon examination of the overall airplane's L/D ratio, it was discovered that in its flight configuration, of 10 m/s cruise velocity and its corresponding 3.75° incidence angle, the aircraft would have a L/D = 13.1 which is 95% of its maximum value of 13.87, as shown in Figure 4.4b. This percentage was deemed acceptable to the design group since neither of the aforementioned concessions were desired.

Some additional characteristics of the Nood Rider 821™'s design are its 0° twist, and absence of both dihedral and sweep. No twist was deemed necesary since the lift distribution was satisfactory and the resulting construction time involved would be excessive. Since the Nood Rider 821™ is equipped with ailerons, no dihedral is needed in order to complete turns. And no sweep angle was desired since the design group wanted every part of the wing to "see" the maximum freestream velocity. This completed the wing design for the aircraft. Next, a drag computation for the aircraft and all its individual components was required.

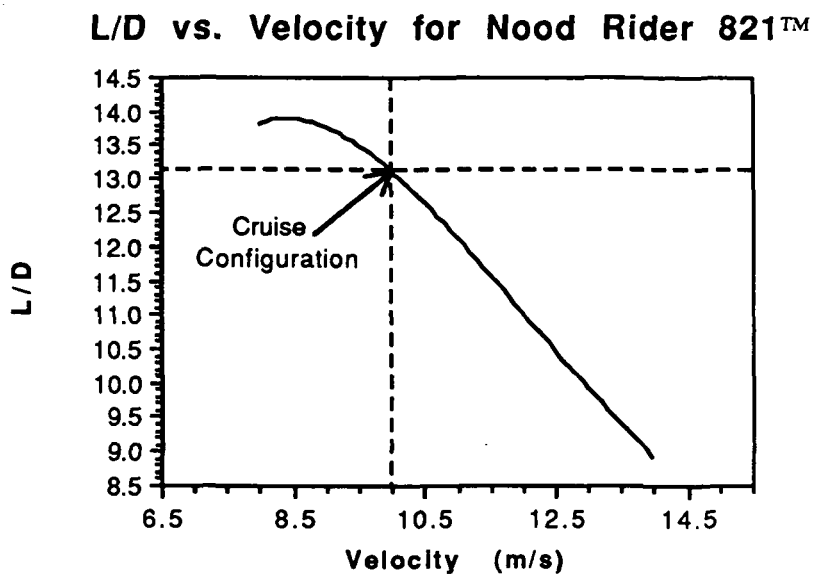

Figure 4.4a

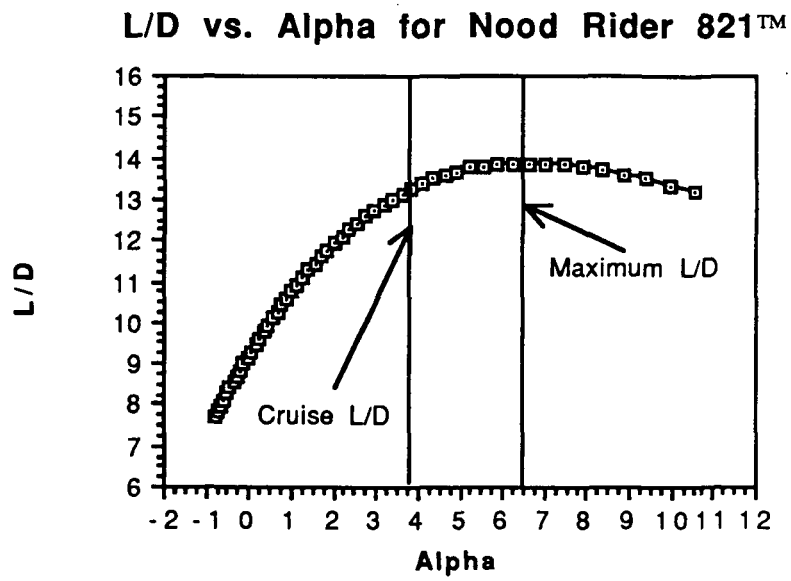

Figure 4.4b

4.3 Drag Prediction

Drag prediction for the entire aircraft was based on a parabolic relationship with lift. This relationship between the coefficient of drag and the coefficient of lift is given in Equation 4.1. Parasitic drag, C_{do}, was estimated using the Subsonic Drag Breakdown method as shown in Appendix A. Using this method, the aircraft was broken down into its major components (wing, fuselage, tail). The total wetted surface area of each component was calculated. The contribution of

each component to the overall drag was calcuated using $C_d = .0055*(A_i/A_{ref})$, where .055 is the skin friction coefficient, A_i is the area of the component, and A_{ref} is the wing area. Next, the drag due to pressure drag was estimated using Hoerner. Compatible components for our nacelles and landing gear were found in Hoerner. Finally, and additional 15% was added to the overall drag to account for interference and imperfections that are bound to occur in drag prediction. The value for C_D as determined using this method is 0.0298.

$$C_D = C_{Do} + \frac{C_L^2}{\pi AR_w e} \qquad 4.1$$

The drag polar for the entire aircraft resulting from the above equation is shown in Figure 4.5

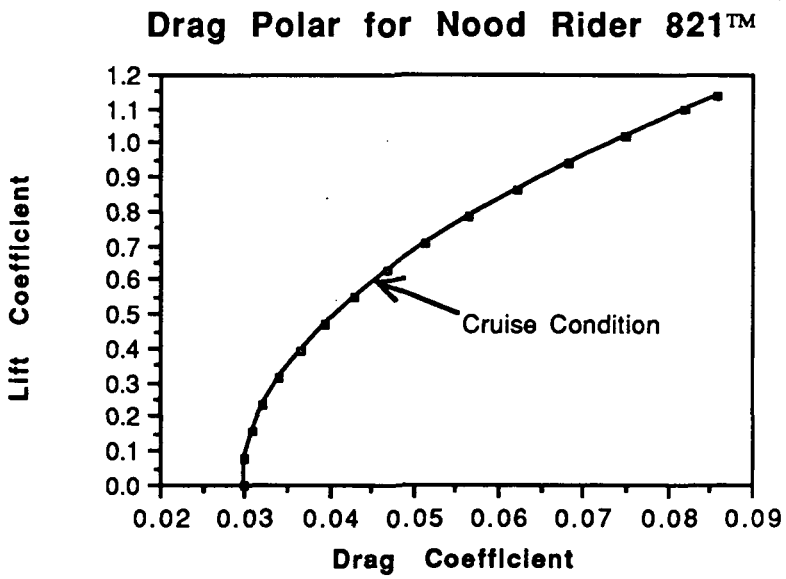

Figure 4.5

The only other aerodynamic specifications not mentioned yet are the lifting characteristics and shape considerations.

4.4 Lifting Characteristics and Shape Considerations

Using J. D. Anderson's Introduction to Flight, and the computer programs Linair 1.4 and Microsoft Excel 2.2a, the lifting characteristics of the Nood Rider 821™ were approximated. The efficiency was calculated using the value given by Linair 1.4 for the wing and tail combination. The contributions of the fuselage and other parts of the plane were then added in using the Subsonic Drag

Breakdown Method to determine the efficiency factor for the entire aircraft. The efficiency factor for the entire aircraft using this method was e = 0.87. The lift curve slope of the airfoil was then corrected for finite effects using Equation 4.2.

$$a = \frac{a_o}{1+\frac{a_o}{\pi A r_w e}} \text{ rad}^{-1} \qquad 4.2$$

The value calculated using this equation is C_{l_α} = 4.487 rad^{-1}. The angle of zero lift, $\alpha_{L=0}$, stayed the same with a value of -4.0°. In order to complete the lift curve for the entire airplane, a method for predicting the stall angle was researched. Linair 1.4 was the eventual method employed to predict stall. The wing and tail configuration was run through angles of attack up to 12° with a wing incidence angle of 3.75°. At every .5° the section lift was plotted versus spanwise position. Sections of the wing started experiencing C_l values of 1.4, the section $C_{l_{stall}}$, at 7°. Seven degrees was then taken as the aircraft's α_{stall}. For angles of attack above the stall angle, the remaining C_ls not above 1.4, were averaged over their lifting surface until 50% of the wing had stalled at 9°. Using Equation 4.3, the zero lift angle of -4° and the finite lift slope, the finite C_Ls were calculated through 12.75°. In doing this, $C_{L_{stall}}$ was found to be 1.14.

$$C_L = a(\alpha - \alpha_{L=0}) \qquad 4.3$$

A graphical analysis can be seen in Figure 4.6. $C_{L_{cruise}}$ for the aircraft is, as indicated, 0.597.

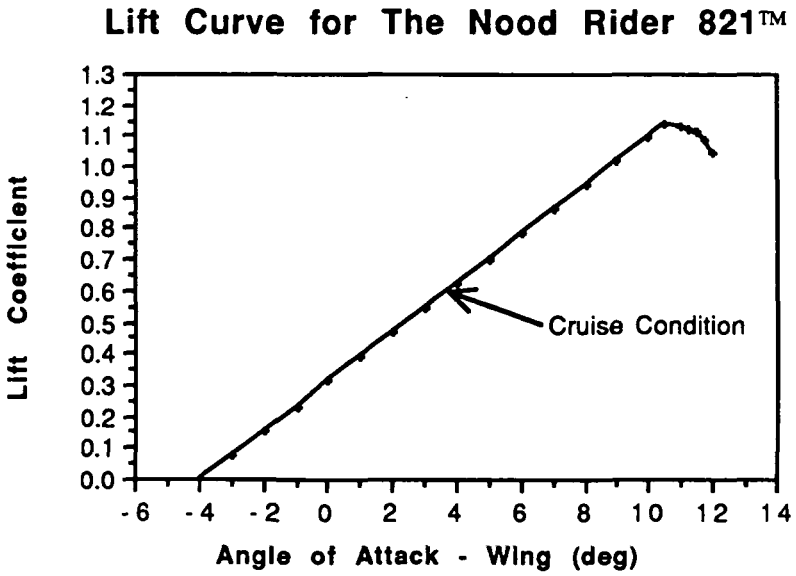

Figure 4.6

Shape considerations were given to the fuselage, landing gear, and engine pylons. The fuselage was tapered fore and aft to reduce form drag. The group decided to utilize a round fuselage mainly due to passenger comfort; however, this decision also yielded a substantial aerodynamic drag savings. The landing gear was kept as short as possible so as to reduce the parasitic drag associated with it. Our desire is to fabricate the landing gear out of a flat, sheet-like material in order to increase the finess ratio of the posts. This will help to reduce the form drag. The same consideration was given to the engine pylons. The only way to reduce the form drag, short of constructing the pylons out of an airfoil shape, was to increase the finess ratio. We have achieved this by using aluminum, thin relative to its chordwise dimension. The airfoil shape is more desirable; however, difficulty in construction outweighs the aerodynamic benefits. The final aerodynamic considerations in design construction was the use of body fillets around all body junctions (i.e. wing connected to fuselage), in order to reduce interference drag.

5. STRUCTURES

5.1 V-N DIAGRAM

The V-n diagram (velocity vs. the load factor) for the Nood Rider 821™ is shown in Figure 5.1. The speed of sound in Aeroworld is 10.67 m/s, since we do not experience sonic effects in Aeroworld up to Mach 1 our maximum velocity is 10.67 m/s. The loading factor of two corresponds to a comfortable loading factor for passenger aircraft. Although we will not experience gusts flying indoors, the gust curves shown on the V-n diagram for gusts of 3 m/s indicate that gusts below five m/s are not a major factor. The factor of safety was chosen to be two due to the inaccuracies inherent in the calculations due to assumptions and the realities of material property variation.

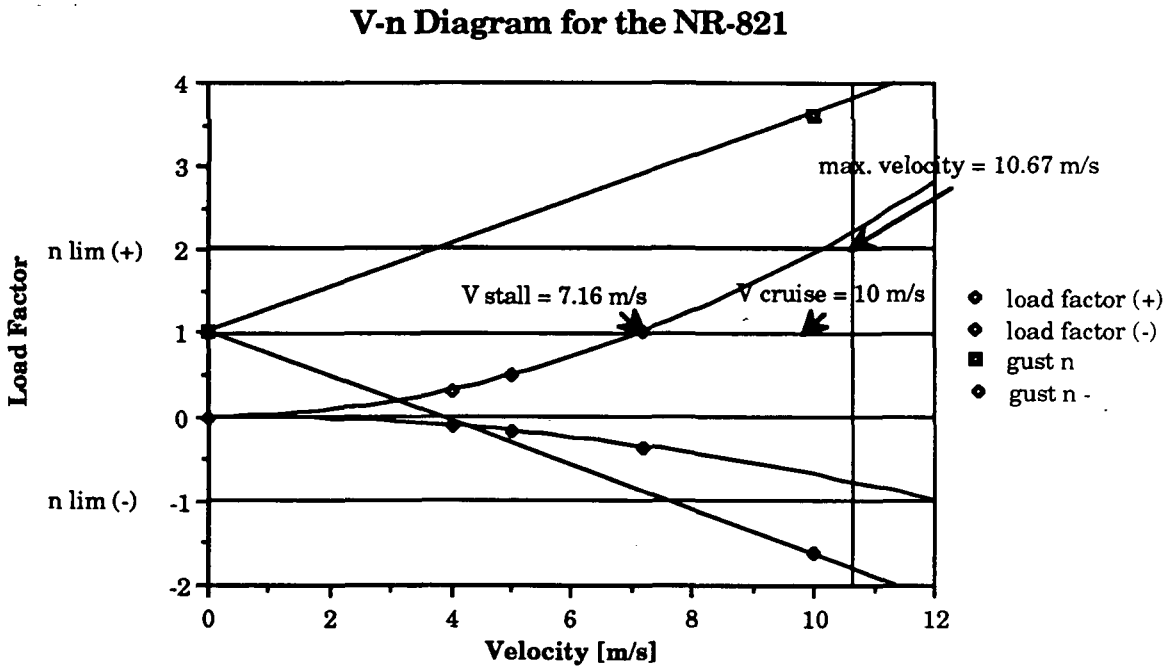

Figure 5.1

5.2 Fuselage

Our initial structural design was set in accordance with our chosen passenger load and the flight requirements. In planning for a pressurized aircraft, our prototype has a fuselage with a circular cross-section. The diameter of this cross-section was determined by the necessary volume of our payload. With each ping-pong ball having a volume of 28.9 cubic centimeters, our total occupancy of 50

passengers requires at least 1445.0 cubic centimeters. In allotting each passenger a travel space equal to twice their own volume, we came up with an internal volume of 2895.6 cubic centimeters.

With this rough volumetric estimate we planned to seat three ping pong balls per row, with an aisle for direct access to the restrooms. Noting that the diameter of each passenger is 2.54 centimeters, our fuselage diameter was set at 19.05 centimeters to meet these design goals. We require 17 rows to fit our maximum capacity of 50 passengers. Giving our passengers what we feel is ample room, a payload compartment of 76.2 centimeters in length was necessary. Taking this into account, along with space for the avionics and the empennage attachment, we set our fuselage length to 107 centimeters. This interior design is shown in figure 5.2 below.

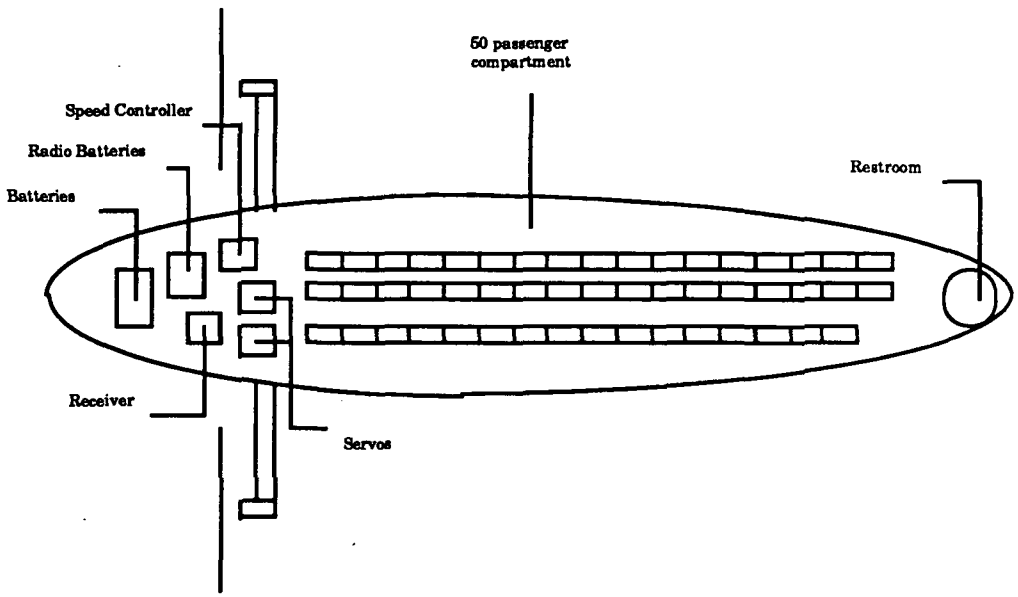

Figure 5.2

The fuselage design was based on strength and weight. We wanted a light weight structure capable of withstanding the forces imposed on it by the horizontal and vertical tail. In order to maintain the shape of our fuselage we used circular ribs, ranging from a diameter of 19.05 centimeters down to 7.62 centimeters at the nose and tail where the airplane tapers. Behind the wing the ribs are placed 7.62

centimeters apart, until just before the tail section, where the ribs are 5.08 centimeters apart for added support. We used a total of 18 ribs for support.

Four main spars attached to these ribs at 0, 90, 180, and 360 degrees, will endure the applied stresses in the fuselage structure. These spars will run the length of the aircraft along with 8 longerons to help in shape and support. The sizing of these spars was done using a stress analysis method, in an attempt to minimize the weight. Researching data on fuselage support sizing from previous years' RPV designs, we came up with an initial range for our spars. The thickness ranges from .159 cm to .635 cm and the range for the spar width is .635 cm to 1.905 cm. Table 5.1 is a spreadsheet listing different sizes and materials for the 4 spars along with the calculated direct stress and weight. The direct stress was calculated using the advanced beam theory for a heterogeneous beam at constant temperature:

$$\sigma_{xx} = -(E/E_1)M_z\, y / I_{zz} + (E/E_1)M_z\, y / I_{zz} \qquad 5.1$$

In determining the direct stress on the fuselage we assumed that the spars in the fuselage would carry the total load from both the horizontal and vertical tail. We modeled the spars as cantilevered beams, from the center of gravity. The force from the horizontal tail is 2.002 newtons, and 3.603 newtons is the force from the vertical tail. This gave us a moment about the y axis, M_y = 1.485 N-m. and a moment about the z axis, M_z = 2.672 N-m. The direct stress can then be solved for using the previously listed equation.

The two materials considered, balsa and spruce, have the following properties:

	ρ (kg/m^3)	E	$\sigma_{xx\ max}$
balsa	5.158	65000	2.7 x 10^6 N/m^2
spruce	13.754	1.3 x 10^6	42.7 x 10^6 N/m^2

We want the lowest weight design that does not exceed the listed allowable stresses. From the resulting data listed, Design 1, made of spruce with a cross-sectional area of .635 cm. by .318 cm., best fits our requirements. Though balsa has a much smaller density than spruce, the cross-sectional area of this material would have to be larger not to exceed the allowable stress. As shown by design 4, this increase in area results in a greater weight for that design.

Design	1	2	3	4	5
Material	Spruce	Spruce	Balsa	Balsa	Spruce
Spar Thickness (cm)	0.318	0.318	0.318	0.635	0.159
Spar Width (cm)	0.635	1.270	1.905	1.270	1.905
Spar Area (cm^2)	0.202	0.403	0.605	0.806	0.302
Iy = Ix (cm^4)	35.4	70.86	106.5	137.011	54.11
Stress (N/m^2)	8.9×10^6	4.47×10^6	2.97×10^6	2.31×10^6	848.41×10^6
Weight (Newtons)	.374	.747	.406	.542	.56

Table 5.1

The nose of the aircraft will be removeable to allow for access to the batteries and avionics. Since the nose, ahead of the engine mounts and wing, has little stress, we designed the lower half to be removeable. This will provide direct entrance to the lower half of the aircraft where all of the avionics and batteries are held in place by strips of Velcro. The Velcro will allow us to place the batteries where they need to be to ensure static stability, and to make quick adjustments if necessary. The nose will be attached by pegs that slide into the fuselage to carry all of the stress and a clip to hold the nose in place. This design creates little extra weight because the extra rib and pegs are made of balsa and are very small.

5.3 Engine mounts

The engines are mounted on pylons located 8.255 cm from the outer edge of the fuselage. The pylons are made of a single aluminum bar measuring thirty five and a half centimeters in length, five centimeters in width, and twenty four

hunderdths of a centimeter in thickness. The length and width were set by the size of the propellers and the spacing of the fuselage ribs, respectively. The material and thickness were determined by the amount of stress a material could carry, the deflection of the pylon, and the stiffness of the material. In addition to the two materials listed above, aluminum was also considered as a viable material. The material properties of aluminum are: density = 2767.91 kg/m^3, Young's modulus = 68.9 x 10^9 N/m^2, and maximum shear stress = 1.37 x 10^8 N/m^2. Using a spread sheet similar to the one used in the fuselage stress analysis we determined the material and the thickness of the pylons.

The forces on the pylons are the weight of the engines and pylons and the thrust produced by the engines. The weight of the engines is multiplied by the maximum load factor (2) and again by a factor of safety of two giving a total loading upon impact of landing of four and a half Newtons per engine - Only one side was modelled due to symmetry. The total thrust was 6.672 Newtons. The moments on the pylons were M_y = .344 N-m about the y axis and M_z = .551 N-m about the z axis. The stress can be evaluated using the same equation:

$$\sigma_{xx} = -(E/E_1)M_z\, y / I_{zz} + (E/E_1)M_z\, y / I_{zz} \qquad 5.1$$

The spread sheet is shown in Table 5.2. The tip deflection is the overriding factor in materials selection. The tips must not deflect more than one half of an centimeter upon impact of landing to insure that the propeller will not come into contact with the ground or the fuselage. The pylon must be made of a stiff material to prevent excessive vibrations from shaking the aircraft and the passengers apart. Aluminum provides the stiffness, support, and repeatability for all of these needs. At twenty four hundredths of a centimeter, aluminum deflects four tenths of a centimeter upon the impact of landing, insuring the safe operation of the aircraft over a number of years.

5.4 Wing

The initial sizing of our wing came from a weight analysis of previous data. We set our wing to a size capable of supplying the necessary lift to overcome this estimated weight. We designed a wing with no sweep, taper or dihedral. As our design progress our weight estimations became more accurate and thus our

	1.5875 mm	2.38125 mm	3.175 mm	6.35 mm
width	0.0508	0.0508	0.0508	0.0508
thickness	0.0015875	0.00238125	0.003175	0.00635
area	8.0645E-05	0.00012097	0.00016129	0.00032258
Izz	1.7343E-08	2.6014E-08	3.4686E-08	6.9372E-08
Iyy	1.6937E-11	5.7161E-11	1.3549E-10	1.0839E-09
E - Al	6.9447E+10	6.9447E+10	6.9447E+10	6.9447E+10
E - Balsa	451402881	451402881	451402881	451402881
E - Spruce	9.028E+9	9.028E+9	9.028E+9	9.028E+9
density - Al	89506.559	89506.559	89506.559	89506.559
density - balsa	5191.38042	5191.38042	5191.38042	5191.38042
density - spruce	14321.0494	14321.0494	14321.0494	14321.0494
stress	24955521.7	7693041.57	3421988.3	579022.585
Aluminum				
tip deflection	0.02410985	0.00714366	0.00301373	0.00037672
defl. n=2	0.048299	0.01431082	0.00603738	0.00075467
Balsa				
tip deflection	3.7092	1.0990	0.4637	0.0580
defl. n=2	7.4306	2.2017	0.9288	0.1161
Spruce				
tip deflection	0.1855	0.0550	0.0232	0.0029
defl. n=2	0.3715	0.1101	0.0464	0.0058
Weights:				
Balsa	0.149	0.223	0.298	0.596
Aluminum	2.567	3.850	5.134	10.267
Balsa	0.149	0.223	0.298	0.596
Spruce	0.411	0.616	0.821	1.643

Table 5.2

necessary lift was altered. Our final wing design holds the following characteristics:

$S = 78.038\ m^2$
$b = 2.134\ m$
$c = 25.4\ cm$
$AR = 8.4$

In the structural design of the wing, once again our main concerns were strength and weight. In researching data from old RPV's, we came up with an initial design of three spars. One leading edge spar, a trailing edge spar and a spar at the quarter chord point. In selecting the material make-up and sizing of this quarter chord spar we used a spread sheet quite similar to that used in the fuselage stress analysis.

The forces resulting in moments over the root of the wing are lift and drag. The lift force per wing is equivalent to half the total weight of the aircraft, $W_{tot} = 21.339$ Newtons, multiplied by the limit load factor, $n_{lim} = 2$. With the moment arm equal to one quarter of the span, the resulting moment is, My = 11.385 N-m. The moment caused by drag is much smaller, but still significant. Using a maximum lift coefficient of, $C_l = 1.1$, and $C_{do} = .0298$, our total drag coefficient was calculated, $C_D = .0865$. For a maximum velocity, v = 10.67 m/s, the drag force on the wing was found to be, D = 3.3 Newtons. Assuming the same quarter span moment arm the resulting moment is, Mz = .871 N-m. These values were used along with the moments of inertia found for the spar in the previous listed equation for direct stress. Table 5.3 lists the resulting stress and weight for different spar designs.

From the results listed in Table 5.3, we chose Design 1, a spar made completely of spruce. The cross-section of the spar cap is a square with .476 centimeters side length. The spar web has a thickness of .079 centimeters, and is 3.81 centimeters in height corresponding to the maximum thickness of the airfoil. This design met the necessary stress requirements and had the lowest weight.

5.5 Empennage

The sizing of the horizontal and vertical tail structures was based on the necessary area for control surfaces. The horizontal tail was designed as a flat

plate. Construction of a horizontal tail with an airfoil cross-section would be quite tedious and not worth the

Design	1	2	3	4	5
Cap Width	.381 cm	.635 cm	0.318 cm	0.635 cm	0.476 cm
Cap Thick.	0.381 cm	0.635 cm	0.318 cm	0.635 cm	0.476 cm
Web Thick.	0.079 cm	0.079 cm	0.159 cm	0.159 cm	0.159 cm
Web Height	3.81 cm	3.81 cm	3.81 cm	3.81 cm	3.81 cm
Cap Area cm^2	0.101	0.403	0.101	0.403	0.210
Web Area cm^2	0.303	0.303	0.652	0.652	0.652
Izz (cm^4)	1.349	17.207	2.077	3.521	2.735
Iyy (cm^4)	0.064	0.626	0.154	0.783	0.133
Material:					
Spar Cap	spruce	spruce	spruce	spruce	balsa
Web	spruce	balsa	spruce	balsa	spruce
Stress (N/m^2)					
Cap ($x10^6$)	38.3	73.0	16.3	75.4	.9
Web ($x10^6$)	42.0	4.4	18.1	4.6	20.7
Weight (N)	.467	.848	.748	.951	.712

Table 5.3

minimal aerodynamic advantages. The horizontal tail has the following characteristics:

$S = 7.74\ m^2$ $\quad AR = 4.8$

$c = 12.7$ cm $\quad b = 60.96$ cm

The vertical tail is tapered to cut down on the drag force. The vertical tail is characterized by:

$h = 20.32$ cm

$c_{root} = 15.25$ cm $\quad c_{tip} = 7.62$ cm

The layout for both the horizontal and vertical tail was based on ease of construction. The horizontal tail is a flat plate with 3 spars and 12 ribs. The ribs are placed one every 5.08 cm to maintain shape.

For the stress analysis of the empennage we ignored what was found to be an insignificant drag force. Therefore, our direct stress equation reduces to:

$$\sigma_{xx} = -(E/E_1)M_z\, y / I_{zz} \qquad 5.2$$

The forces on the empennage were previously listed as, 2.0 newtons from the horizontal tail, and 3.6 newtons on the vertical tail. Using our stress analysis technique with this new stress equation, we came up with a horizontal tail spar cross-section of a quarter of an inch. This structure has the strength to withstand the maximum direct stress, 1.79 MPa, that was calculated. The vertical tail is subjected to almost twice the force as the horizontal tail and therefore was built using spruce for the extra strength. The vertical tail has the same .635 centimeter cross-section as the horizontal tail (See Appendix B1 for calculations).

5. 6 Weight Estimation

The first major task for the structures group was to come up with a reasonable estimation for the total weight of our design. A weight estimation would give us a value for the necessary lift. Both the propulsion and aerodynamics groups required this information for engine and airfoil selection. We had already determined the approximate size of our aircraft from a 50 passenger capacity volume estimation. We used this initial size in comparison with old RPV weight data. Although the RPV's from the previous year were much smaller in size than our design, we came up with an acceptable weight estimation. The avionics we used were similar to last years, and thus their weight was assumed the same. We also had to account for the excess weight of two motors.

As our design analysis progressed, our weight estimate became more accurate. After viewing a full size sketch of our initial plane, we made some structural changes. The nose and tail sections on the fuselage were tapered at a smaller angle, cutting down on both aerodynamic drag and structural weight. A redrawing of this new design showed a well proportioned, aerodynamically contoured aircraft.

COMPONENT	WEIGHT (Newtons)
PROPULSION COMPONENTS:	total weight: 4.95
Engines	4.58
Propellers	0.33
STRUCTURAL COMPONENTS:	total weight: 8.55
Engine Mount	1.17
Wing	3.20
Horizontal Tail	0.61
Vertical Tail	0.18
Fuselage Layout	1.45
Forward Landing Gear	1.53
Rearward Landing Gear	0.42
AVIONICS:	total weight: 7.21
Batteries	3.98
Servos (all 3)	0.50
Receiver	0.28
Speed Controller	0.96
Radio Battery	1.53
PASSENGERS: (50)	1.23
TOTAL WEIGHT:	21.97 newtons

Table 5.4

Our different subgroups began making decisions which allowed us to pinpoint the total weight. The propulsion group chose a motor, propeller and the battery necessary to run these. We were able to get exact weights for these chosen components from data provided by their manufacturer. The stability and controls group came up with the necessary sizing of control surfaces to maintain aircraft stability. From this sizing we determined the volume of the structural components needed to secure the control surfaces. Using the known material density, along with these volume estimations, we calculated the weight of the structural components.

Table 5.4 lists the final weights for the different components making up our aircraft. The table is separated into avionic, structural components and propulsion. The weight of the different structural components was found by

using volume estimations along with the density of the material. The avionics were weighed and thus these values are precise. The weight of the propulsion components was provided by the manufacturer as data.

5.7 Center of Gravity Estimation

In order to ensure aircraft stability, we wanted our center of gravity to be as close to the aerodynamic center of the wing as possible. Once we had reliable weight estimations we were able to calculate the individual center of gravity for all of the components less the avionics. The placement of the avionics was left for us to determine. Figure 5.3 shows the location of all the aircraft components, with the avionics listed below the mid-line of the plane. Excluding the internal components, we came up with an overall center of gravity location approximately 35.56 cm behind the nose of the aircraft. This cg location is unstable, being over 3.81 cm behind the aerodynamic center. We therefore used our avionics to push the cg forward.

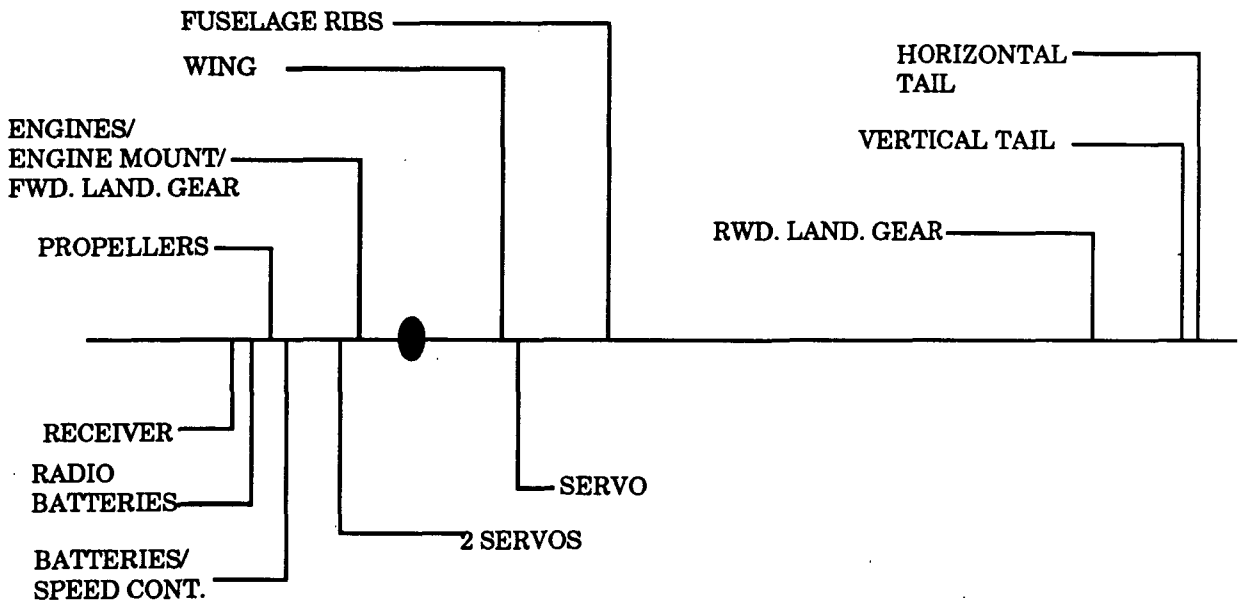

Figure 5.3

Our internal components make up over 35% of our overall weight and thus their placement is quite significant in the cg location. The only restrictions on avionics placement was on the servos. The servos were positioned for access to control surfaces. The remaining components were placed in the front of the fuselage to shift the cg forward. From this positioning, the design center of gravity was

found at 29.21 cm behind the nose. Table 5.5 lists the weights and center of gravity locations for all the individual components of our design. The resulting center of gravity location is just ahead of our aerodynamic center and optimal for stability and control. We placed our battery pack on balsa wood 'tracks' and secured them with rubber bands. This is secured to the main aircraft through the use of pegs. This allows us to be able to manipulate our cg placement by simply moving the battery pack system.

COMPONENT	**WEIGHT** (Newtons)	**CENTER OF GRAVITY** (cm behind nose)
Engines	4.58	23.50
Engine Mount	1.17	23.50
Propellers	0.33	18.42
Wing	3.20	36.07
Horizontal Tail	0.59	102.87
Vertical Tail	0.18	101.85
Fuselage Layout	1.45	47.0
Forward Landing Gear	1.53	23.50
Rearward Landing Gear	0.42	91.44
Passengers	1.22	53.34
Resulting weight & CG:	14.70	36.58
AVIONICS:	total weight: 24.1	
Batteries	3.48	8.89
2 Servos	0.33	23.50
1 Servo	0.17	35.56
Receiver	0.28	12.19
Speed Controller	0.92	17.78
Radio Battery	1.53	17.78

Table 5.5

Design Center of Gravity

$$X_{cg} = \Sigma \text{ (Weight * C.G.)} / \Sigma \text{ Weight}$$

$$X_{cg} = 29.21 \text{ cm behind the nose}$$

6. PROPULSION

6.1 Motor Sizing

The first major deliverable item on the Nood Rider 821™ was the engine itself. Therefore, it was necessary to pick a motor based on the preliminary sizing of the aircraft. We felt that the flight regime which should be used to select the motor would be takeoff, as that regime would require the most power. We limited our choices to the Astro Cobalt motors based on the experiences of past design groups and their good reports concerning the performance of these motors.

The preliminary sizing of the aircraft involved a fairly low value of $C_{L_{max}}$, which caused our calculated takeoff velocity to be quite high. The large value of takeoff velocity propagated through the takeoff power required calculations (as can be seen in Appendix C, equations 1-3), and gave us required power values ranging between 85 and 140 watts. These seemed on the high side of reasonable to us, but we definitely wanted to have sufficient power to takeoff.

One of the things which makes the Nood Rider 821™ different from all the other airplanes in its class is the fact that it is the only one that is being built on the twin engine concept. This, therefore, allows us to require only half the power necessary to be produced by each engine, or in this case, between 42 and 70 watts per side.

The last characteristic which we had to take into account when sizing the motor was the efficiency of all the components through which the propulsive forces would travel before they would actually move the airplane. The motor, the gear, and the propeller all would contain some inefficiencies which would have to be corrected for. Our initial estimates suggested that we could count on a minimum of 50% of the power transmitted from the motor to be available for propulsion, thus all the motor power available figures should be scaled by a factor of 0.5.

Engine Type	Maximum Engine Power
Astro 035	105 watts
Astro 05	125 watts
Astro 05FAI	123 watts

Table 6.1

Of the Astro Cobalt motors available, we looked at three based on the power required figures presented above. These were the Astro 035, the Astro 05, and the Astro 05FAI. Looking at Table 6.1, we can see the maximum power available from each of these three motors. The Astro 035 may have had sufficient power for our application, but just barely. The Astro 05 and the 05FAI have very similar power outputs, with the 05 being just a little higher with there being no motor weight penalty. Therefore, we have selected twin Astro 05 motors, realizing that, while they give us more than sufficient power, the next smallest may have been insufficient for our airplane. Likewise, we recognize that one of the other requirements of our airplane is the ability to be expanded into derivative aircraft, and we feel that these motors will be serviceable on any enlarged version of the current Nood Rider 821™.

6.2 Propeller Selection

Among the primary propeller selection criteria for The Delta Group was the necessity to keep the propeller diameter as small as possible. Because we are mounting our motors on pylons, and because they are of significant weight, we wanted to keep the moment arm as small as possible. Therefore, the smaller the propeller, the shorter the pylon, which will minimize the moment around the body-fixed x-axis, thus making roll control easier.

With this notion in mind, we scoured our data base for information on small diameter propellers. The primary (and only) data on small diameter propellers comes via a program written by Barry N. Young for the Apple IIe computer. This program analyzes propellers using simple blade element theory knowing blade characteristics at specified spanwise positions on the prop. The program allows the user to vary flight velocity and returns three useable characteristics of the propeller: the efficiency versus the advance ratio, the thrust coefficient versus advance ratio, and the power coefficient versus advance ratio. The program itself contains data files covering the geometry of many propellers from 8 inch diameters on up to 13 and 14 inch diameters. Using this program as our basis, we analyzed the smallest diameters available: the 8-4, the 8-6, the 9-4, the 9-6, the 10-4 and the 10-6. We felt that this was a sufficient range of propellers to begin with and if it were determined that these were not powerful enough, more propellers could have been studied.

Figure 6.1 is a graph of the thrust coefficient versus advance ratio for each of the propellers under consideration. The thrust coefficient can be changed into the thrust available through the equation:

$$T=C_T\rho n^2(d_{prop})^4 \qquad 6.1$$

where C_T is the thrust coefficient, ρ is the air density, n is the number of revolutions per second of the propeller, and d_{prop} is the propeller diameter. This yields thrust available curves such as can be seen in Figure 6.2. From these

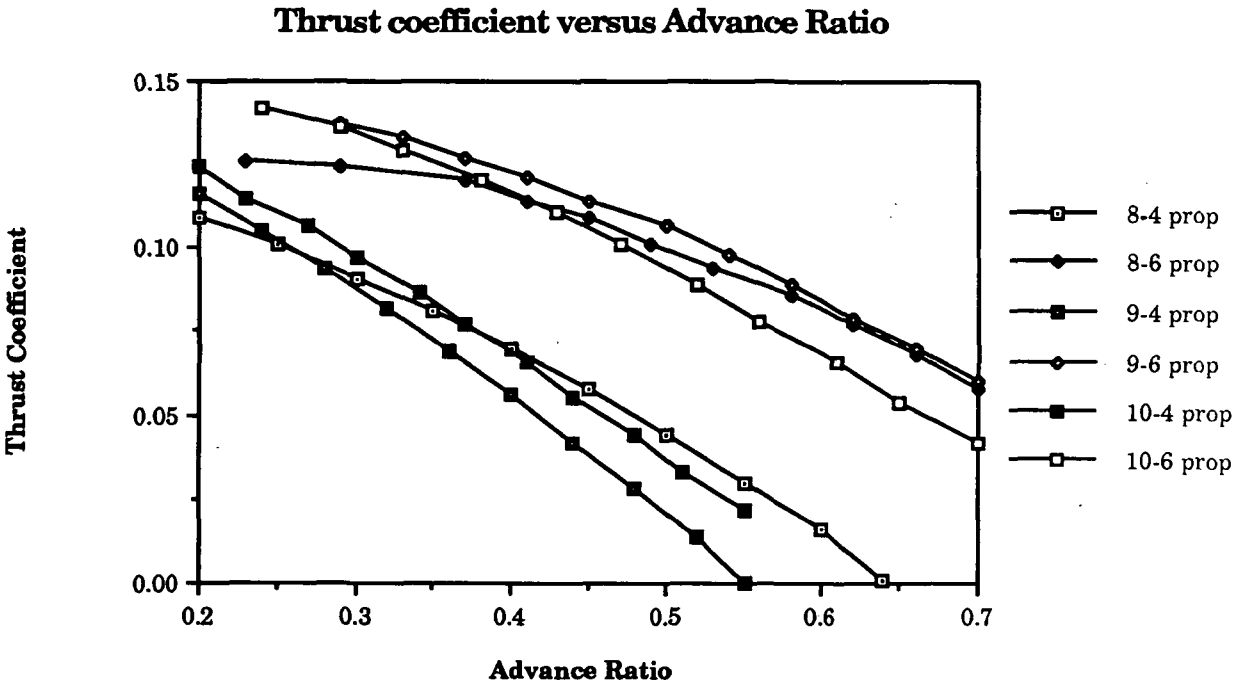

Figure 6.1

curves, it should be apparent that the larger propellers give significantly more thrust than do the smaller props.

At this point in the overall design study, the parameters of the airplane were fairly well defined, so that we were able to know that we had a thrust requirement at cruise of 2.82 Newtons (1.41 Newtons/side) and a thrust requirement at takeoff of 8.39 Newtons (4.19 Newtons/side) (Calculation of takeoff and cruise thrusts was accomplished using the method shown in Appendix C). It was quite obvious that the 8-6, the 9-6, and both of the 10 inch propellers provide far more thrust than necessary, and can be discarded from further study.

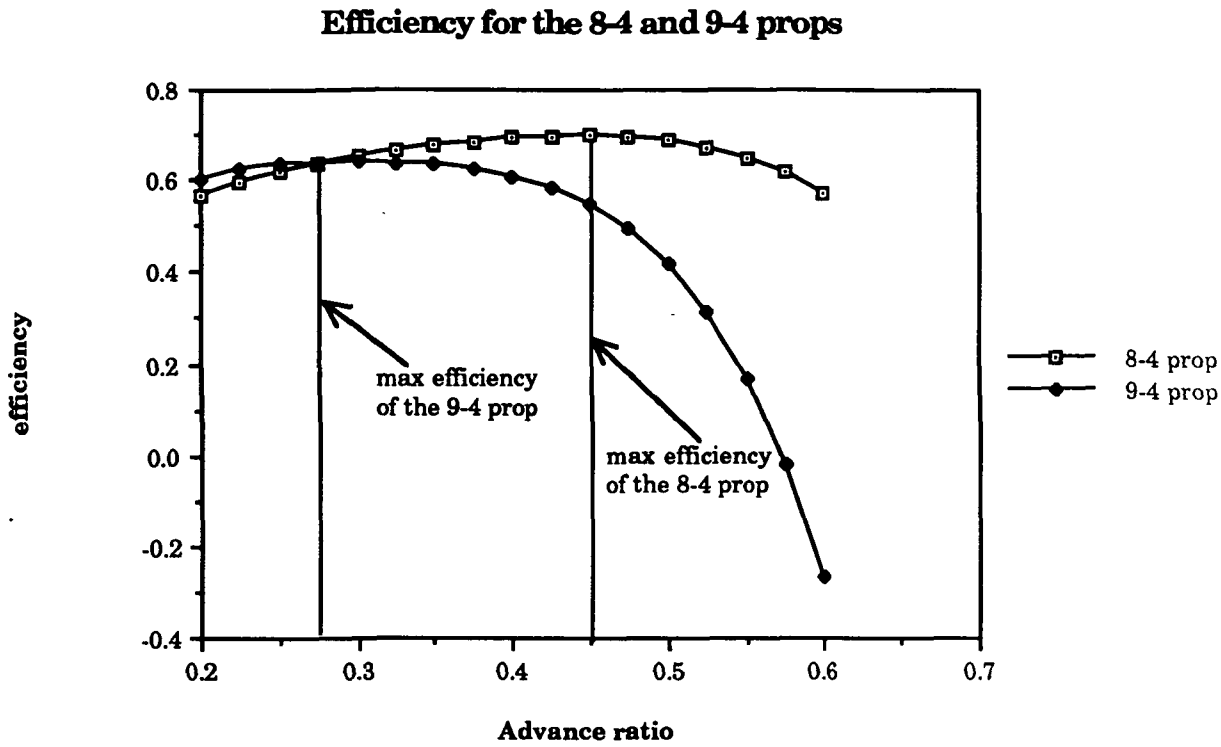

Figure 6.2

Once the number of propellers had become a manageable two, it was time to explore the cruise performance of each. Because of the fact that the greatest portion of the flight will be spent in the cruise phase, we felt that the propeller should be functioning as close to its peak efficiency during cruise. Figure 6.2 shows the efficiency of the two propellers as a function of the advance ratio. Using the chosen cruise velocity of 10 m/s, we attempted to find an advance ratio at which the thrust and power available matched the thrust and power required for each propeller. We then overlaid the maximum efficiency of each propeller and determined which propeller would be functioning closest to peak efficiency at cruise, as can be seen in Figure 6.3. From this graph it is evident that the 8-4

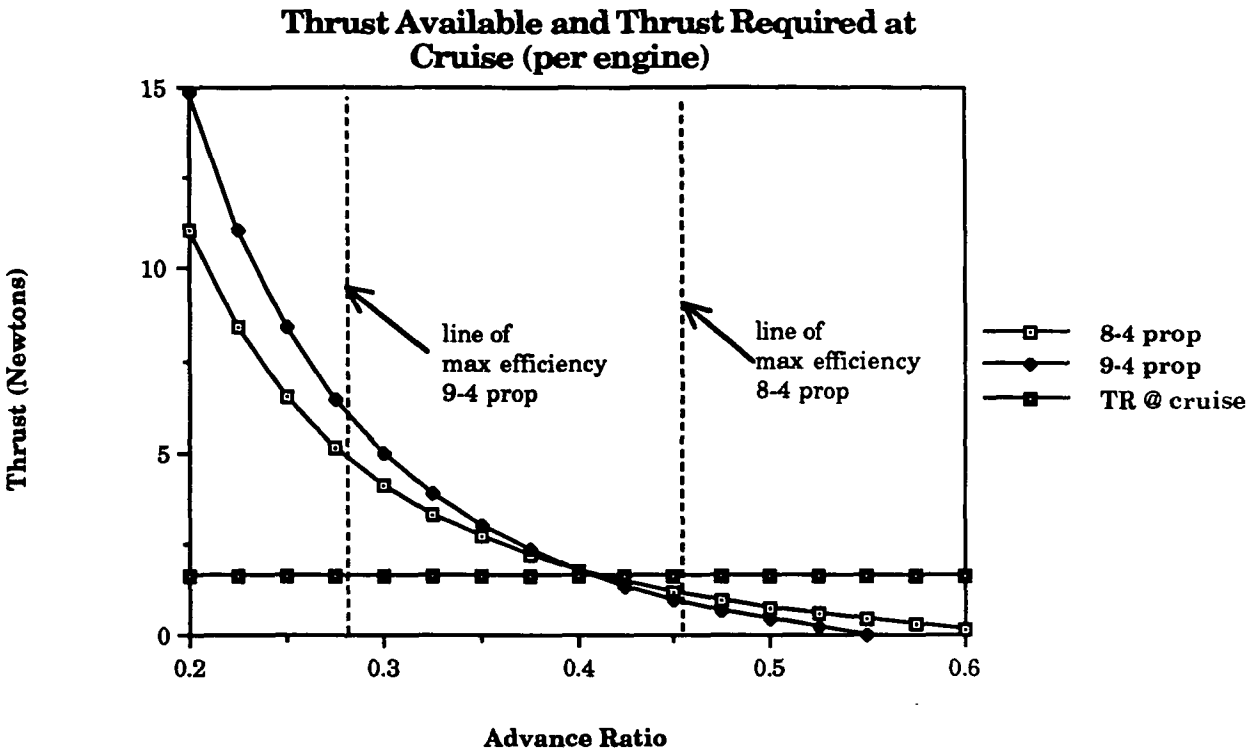

Figure 6.3

propeller is functioning closest to its peak efficiency at cruise, and because we have already determined that it has sufficient thrust for takeoff, it is the propeller of choice for the Nood Rider 821™.

6.3 Battery Selection

Battery selection for the Nood Rider 821™ was based on two primary concerns. The first of these concerns is the capacity required for all the flight regimes as specified by both the *Request for Proposal* and the design requirements and objectives of The Delta Group. The second concern centers on having sufficient battery pack voltage to power the motor in all phases of flight.

The capacity of the battery is a function of the sum of the current drains of each of the flight phases. These can be calculated knowing the torque load on the propeller, given by the equation:

$$Q = \frac{TV}{2\pi n \eta} \qquad 6.2$$

where T is the thrust, V is the velocity, n is the number of revolutions per second, and η is the efficiency of the propeller. Once the torque is known we can use the motor torque constant (K_Q = .61586 in-oz/amp) and the torque loss (Q_L = 1.1246 in-oz) to determine the current drain through the equation

$$I = \frac{Q - Q_L}{K_Q} \qquad 6.3$$

where I is the current. Using these equations, we determined the current drain for each segment of the flight, as listed in Table 6.2.

Flight Phase	Current Draw
Takeoff	16.64 amps
Climb	11.00 amps
Cruise	9.00 amps

Table 6.2

The current drain could then be multiplied by the amount of time spent in each of the flight phases, as calculated knowing the velocity and distance required for each phase. These values would be summed over the entire flight to give us the capacity required. According to the standards set by the *Request for Proposals*, however, we are required to have sufficient battery capacity to loiter for 60 seconds in case of traffic and then be able to fly to an alternate airport to land. Because we

are flying at a cruise configuration where thrust equals drag and lift equals weight, any time required for diversion to alternate airport or loiter would require the same current draw as cruise. Therefore, summing the capacity required over all flight phases, we came up with a total capacity required for the flight of 658 Mah, to which we added 17 mah to deal with ground handling (as the current draw is nominal during this phase) to come up with a total battery capacity of 675 Mah for the Nood Rider 821™.

The second concern is the requirement for sufficient battery pack voltage during all phases of the flight. We will require a battery of the rapid charge, high rate discharge variety, in order that we can satisfy the large current draw at takeoff. For this purpose we have taken into consideration two batteries, the P-120SCRP and the P-90SCRP, both manufactured by Panasonic. We are looking at these two batteries based on the experiences of past groups and the recommendation of the electronics expert at our disposal. The batteries have nominal capacities of 900

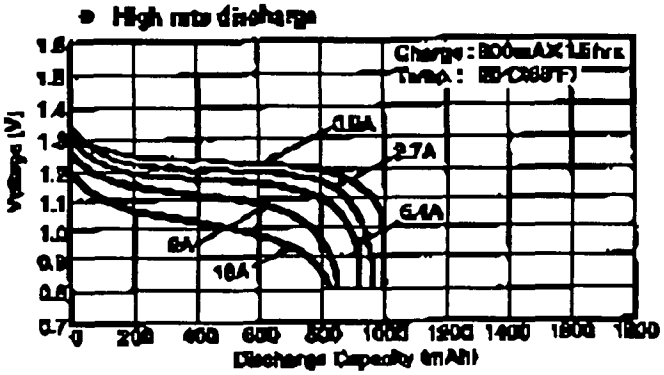

Figure 6.4

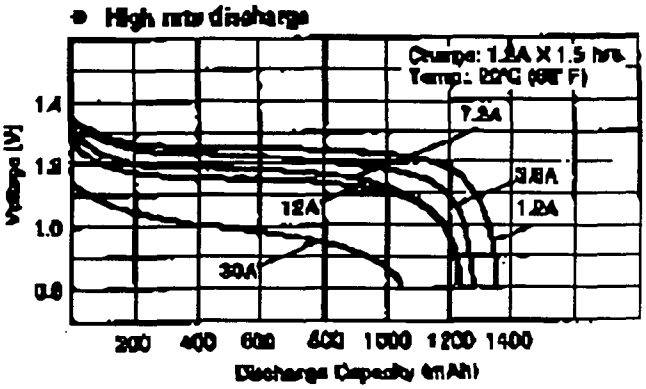

Figure 6.5

and 1200 Mah, respectively for the P-90 and P-120, with nominal voltages of 1.2 volts each. If we look at the discharge curves for each of these batteries (Figures 6.4 and 6.5, respectively, for the P-90 and P-120 respectively), we can see that the actual voltages are somewhat less than the nominal. If we figure a maximum current drain at takeoff of 16.64 amps, and a required capacity of 600 Mah, we can see that the P-120 would have a cell voltage of 1.07 volts, while the P-90 would have a cell voltage of 1.0 volts. We can calculate the actual battery voltage required knowing the battery and armature resistances, and the motor RPM and current

draw at any flight phase, as well as the motor voltage constant (K_V = 4.6721 x 10^{-4} V/RPM) through the equation

$$V=K_V*RPM + I*R \qquad 6.4$$

where I is the current and R is the total resistance. This yields a maximum required voltage of 10.0 volts at takeoff based on a current draw of 8.32 amps, and armature resistance of 0.04 ohms and a battery resistance of 0.07 ohms. Therefore, we can see based these numbers and Figure 2.6 that the Nood Rider 821™ will require 10 P-90SCRP batteries to give sufficient voltage, current draw, and capacity for all phases of the flight.

6.4 Heating Effects

Because we have determined that the mechanical parts of our propulsion system are less than one-hundred percent efficient, we need to look at the heat generated in the components and decide what to do about it. We expect that heating will occur in both the motors and the batteries, and that it can be calculated knowing the current flow and the resistance. The calculation is $Q=I^2R$, where Q is the heat, I is the current, and R is the resistance. With a maximum current draw of 14.4 amps at takeoff and a motor resistance of 0.04 ohms, the motor will dissipate 8.28 watts. Similarly, the batteries, with a resistance of 0.07 ohms will dissipate 14.5 watts of heat at takeoff. The cooling of the motors should be of no problem in that they are mounted on pylons, fully exposed to the airflow for convection cooling. With the batteries, we will probably have to provide slits on the underside of the fuselage to allow for forced convection as the Monokote covering will not allow for sufficient air diffusion for cooling.

6.5 Propulsion System Installation

The installation of the propulsion system into the aircraft will be tricky for several reasons. The first of these is the fact that there will be two motors mounted on pylons. The motors will have to be adequately fastened to the pylons to prevent shear both in flight and upon landing. In addition, the two motors will be hooked up in parallel, splitting the available current while keeping the voltage the same. These will be controlled through an on-board speed controller as we do not wish for the plane to be flying at full power all the time. This speed controller will have to control both motors simultaneously, and keep them at nearly identical power settings in order not to set up a moment around the body fixed z-axis. In order to

prevent a similar moment around the body fixed x-axis, the two motors will be set up so that their propellers will swing counter to one another.

7. STABILITY AND CONTROL

The Nood Rider 821 was designed to fly with a high amount of maneuverability and yet to possess a high amount of stability for ease of cruise condition flying. The aircraft, as designed, is stable about all three axis of rotation. The pitch, roll, and yaw are sufficiently damped to maintain a stable aircraft through all aniticipated flight conditions. The aircraft is also controllable about all three axis of rotation by the use of three control surfaces. These include a(n) elevator, rudder, and counter-actuating ailerons. As the aircraft design was evolving, each individual member of the aircraft was placed on an Excel spreadsheet along with its location and weight. This enabled for calculation of the cg and moments of inertia for all the configurations and control surface sizing.

7.1 Horizontal Tail and Elevator Sizing

The pitch stability of the aircraft was the most studied aspect of stability. From data on previous aircraft, controlling the pitch stability by cg placement was determined to be of great importance and needed to be carefully studied. Many previous designs needed cg shifting during both construction and flight test phases to maintain stability. The sizing of the horizontal tail and vertical tail play a major role in cg placement as they have a large contribution to cg position as well as the attitude control capability.

Initially, 'guesses' were made at the sizes for the tail surfaces from pre-existing models. From these initial guesses, variations were then made and the corresponding shift in cg noted. For sizing of the horizontal tail, the vertical tail was taken to be what was felt to be oversized, since later reduction in its size would be favorable, not unfavorable to cg location.

Studies were then done to determine the most desired horizontal tail size. The chord of the horizontal tail was varied from 3 to 7 inches and the span varied from 18 to 30 inches. Although the larger tail sizes provide for more pitch stability, the cg became unacceptable as it moved behing the wing ac. Span of the horizontal tail was finally place at 24 inches and the chord narrowed to 4 to 6 inches, including the elevator. The aircraft was found to be adequately stable using any size in the 4 to 6 inch range as illustrated in the following moment coefficient vs.

angle of attack graph. The coefficients were determined using LinAir. (A sample LinAir input file is provided in Appendix D).

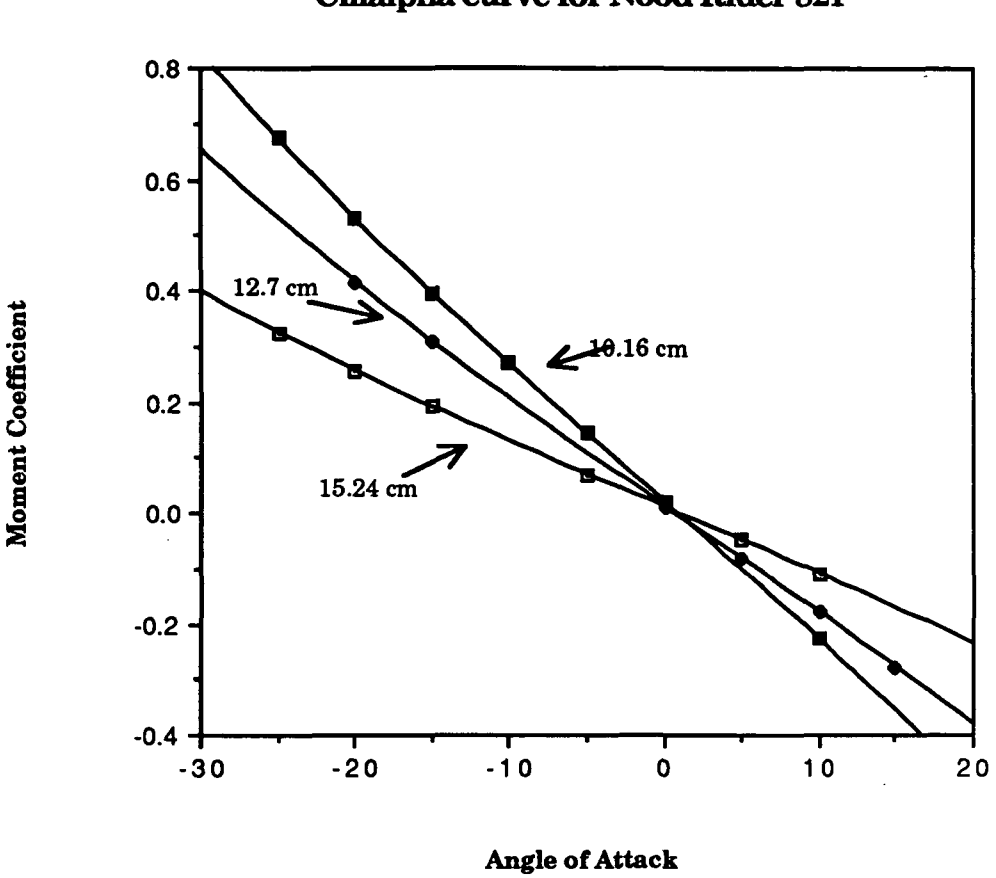

Figure 7.1

The final sizing of the chord became a matter of elevator sizing. It was decided that the final criterion for elevator/horizontal tail sizing should be trying to give the aircraft a damping ratio for level flight that is in the known good handling qualities range. To do this, approximations for determing damping ratios, were taken from Nelson, "Flight Stability and Automatic Control". Also the aircraft was modelled on LinAir and moment coefficients for different elevator deflections determined. The approximations from Nelson and the coefficients from LinAir were then used in a computer code (see Appendix D) to determine the pitch damping for the various elevator sizes. It was found that using a 60.96 cm chord and a 5.08 cm elevator that extended the length of the span, the aircraft had an approximate damping ratio of .52 and a frequency of 1.13 s^{-1}. This falls within the

'good' handling qualities range for the experimental results given in Nelson and should help avoid pilot induced oscillations. This matter is of great concern since the pilot will be flying the aircraft for the first time.

It was then needed to varify that the 5.08 cm elevator provided sufficient power to pitch the aircraft to desired angles of attack and control the aircraft through the flight envelope. Returning to the modelled aircraft on LinAir, the elevator was deflected through a range of deflection angles at various fuselage angles of attack. This produced the elevator power curves seen in figure 7.2.

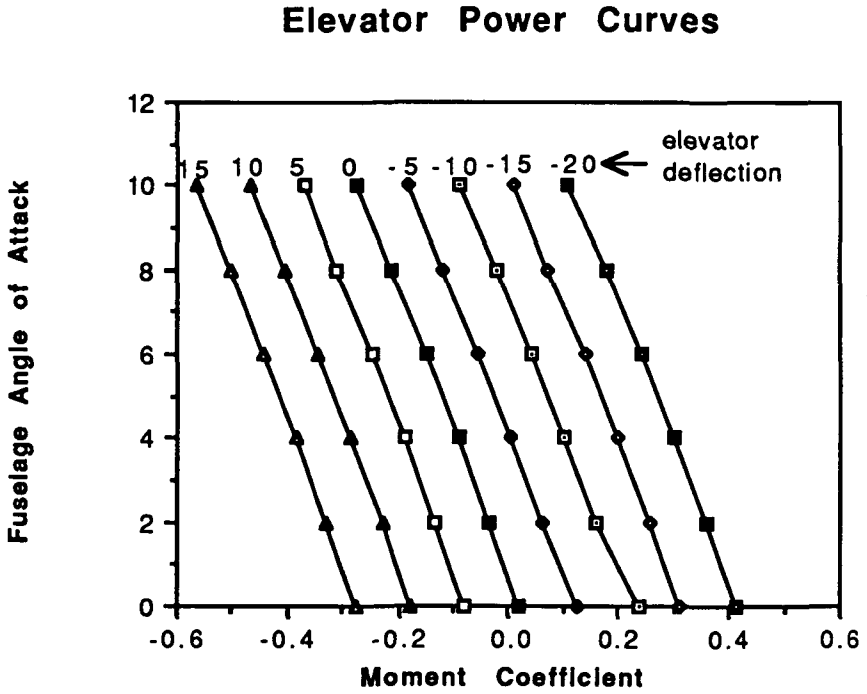

Figure 7.2

From this data it is seen that the 5.08 cm elevator provides adequate pitch control. The aircraft has a moment of inertialabout its y axis of approximately 9.16 kg-m^2. With this moment of inertia, it was determined that a moment coefficient of +/- .1 should be able to be attained at any flight condition to ensure adequate control. The wing of the aircraft stalls at a fuselage angle of attack of 10 degrees. If the elevator is fully deflected to -20, there would still be sufficient power to rotate the aircraft to its highest needed angle of attack. Thus, the elevator will be installed

on the aircraft such that it is able to deflect 25 degrees in either direction, in order to provide for a margin of safety. It is also noted that with the elevator in its nuetral postion with no deflections, the moment coefficient is approximately equal to zero so that the aircraft can be trimmed with no elevator deflection.

7.2 Vertical Tail and Rudder Sizing

With the elevator sized, the next control surface of concern became the vertical tail and rudder. Of overriding concern in the sizing of the vertical tail was the performance of the aircraft in the event of an engine failure. Since the twin engine configuration was chosen to ensure safety for overwater flights, it was desired to design the rudder such yaw control could be maintained with one engine out. To do this, the rudder needed to be large enough to counter a moment of 3.38 N-m. This moment accounts for the drag of an unfeathered prop and the assymetric thrust of one engine flight as well as the power needed to yaw the aircrafts 9.58 kg-m^2 moment of inertia about its z axis.

It became obious early, that the flap effectiveness parameter would need to be quite large, on the order of .5-.6 in order to control the large moment. Also, the surface of the tail itelf needed to be such that the high amount of directional stability it provided would further aid in engine out flight. After again beginning with an intial 'guess' of the required tail size, the size was changed and its effect on control observed. A tail of surface area .046 m^2 was chosen. Of this area, 44% is rudder. The rudder size was chosen by determining the flap deflection needed to obtain the required moment. With the rudder size as chosen, the rudder can obtain the required 3.38 N-m moment at a deflection of approximately 20 degrees. This can be seen in figure 7.3.

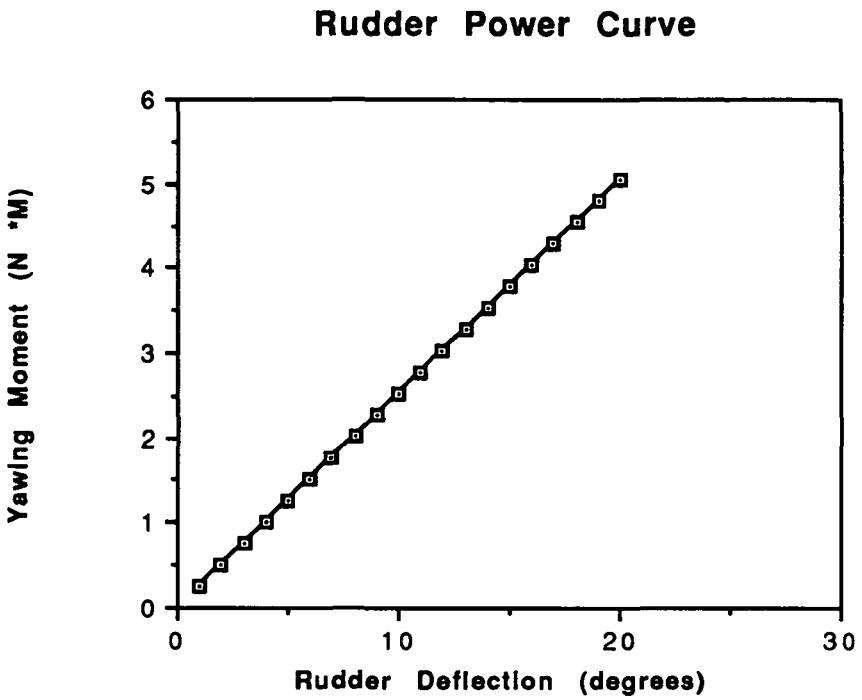

Thus the rudder will be installed such that it can deflect 25 degrees in either direction. A point of concern with the rudder being so powerful is the control of the aircraft during normal operational flight. Deflections on the order of 5-6 degrees will be sufficient to control the aircraft. Although controlling these deflections will be easily controlled on a full scale aircraft, the technology demonstrater me encounter some difficulty allowing the pilot to deflect the rudder to large angles. Thus, on the technology demonstrater, the rudder deflection may be limited if an adequate servo control mechanism is not found.

7.3 Roll Stability and Control

Roll stability of the Nood Rider 821 is achieved by use of a high wing configuration. This high wing gives the aircraft a $C_{lB}<0$. The aircraft will also use the 'induced' dihedral that will happen due to wing bending during flight. The tip deflection at stall cruise will give a wing dihedral of approximately 1 degree. This dehedral in combination with the high wing set up, will provide adequate roll stabiltily.

The roll control of the aircraft will be achieved using counter actuating ailerons on the wings. These are being used to aid the pilot in turning the aircraft as well as maintain wings level flight in the event of an engine loss. The sizing of the ailerons was done by determing the control power needed to roll the aircraft

through a turn radius of less than 5.49 m. It was decided that in order to prevent the aircraft from being overly responsive in turn however, that the ailerons should provide a 'gentle' rolling motion and the pilot should use both ailerons and rudder for coordinated turns. A bank angle of 20 degrees is desired for our turn requirements. It was decided that allowing the pilot to roll the aircraft to that angle in 2 seconds at full aileron deflection. This was purely a estimated time on our part as to what we felt the pilot would be comfortable with.

The aircraft has a moment of inertia of approximately, 3.6 kg-m^2 about its x axis. Using this figure it was detemined using rolling moment approximations from Nelson that airlerons of 2.54 cm chord and a 30.48 cm span placed 60.96 cm out on the wing would be sufficient.

8. ECONOMICS

The Delta Group performed a study on the economic feasibility of constructing and operating the Nood Rider 821™. The main goals of our economic study were to determine the optimum number of aircraft to be produced, the passenger ticket price, and the operating profit. The following is a description of the analysis and the results at which we arrived.

8.1 Production Costs

The first aspect of the economics of the Nood Rider 821™ to be analyzed was the aircraft production costs. The individual subsystems of the aircraft were divided into four subgroups. These subgroups are: avionics, propulsion, structures, and labor. The following list shows the individual costs within each subgroup. (All dollar values are shown in Aeroworld costs.)

Avionics	
Radio & Receiver	$46 400
Servos (3)	39 600
Speed Controller	52 000
Total	$138 000
Propulsion	
Engines (2)	$72 800
Fuel Cells (10)	24 000
Total	$96 800
Structures	
Material (i.e. Balsa, Aluminum)	
Fasteners & Adhesives	
Landing Gear	
Actuating Apparatus	
Covering	
Total	$60 000
Labor	
Construction (80 hours)	$8000
Design	3600
Total	$11 600

Addition of the subtotals gives a total unit cost of $306,400. The labor - design cost is based on the production of 25 aircraft. Figure 8.1 is a graphical view of the relative magnitude of each of the individual subgroups.

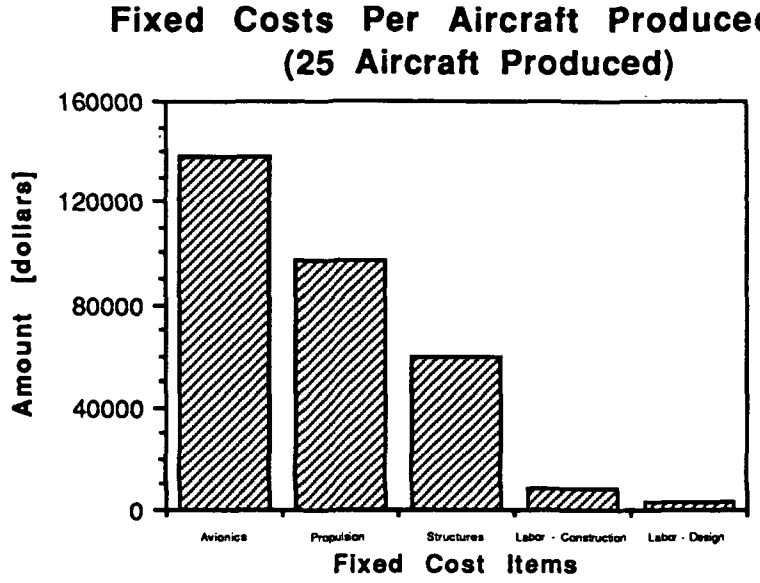

Figure 8.1

A graphical analysis was used to determine the optimum number of planes to be produced. The cost of designing the Nood Rider 821™ is $90,000. This cost can be amortized over the total production run. Therefore, the more planes produced, the smaller the contribution of design cost to the unit cost. Figure 8.2 visually shows the variation in unit cost with the total number produced. After 25 aircraft are produced, the total cost per aircraft levels off. Producing any more aircraft will yield a negligible difference in total aircraft unit cost.

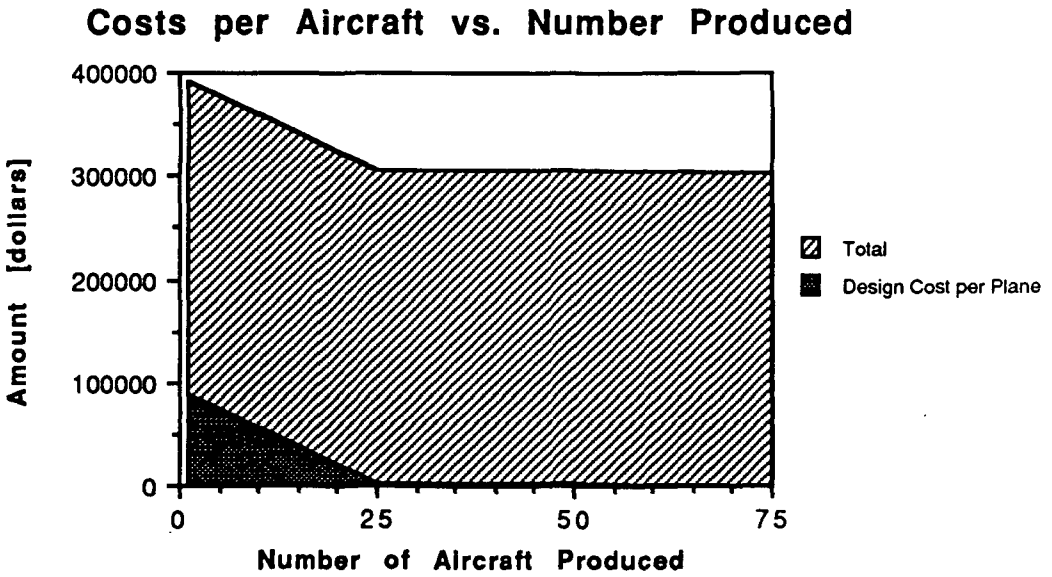

Figure 8.2

The Delta Group, manufacturers of the Nood Rider 821™, intend to reap a profit of approximately 20% per aircraft sold. This brings the total cost per unit to the airlines to $368,000. This price then yields a profit of $63,080 to The Delta Group for each aircraft sold.

8.2 Operating Costs

The second aspect investigated was the operating costs per flight of the Nood Rider 821™. As with the production costs, the operating costs were broken down into subgroups. The five subgroups used are: fuel, maintenance, crew, food & beverage, and equipment cost (depreciation). The cost breakdown is as follows:

Fuel	
433 mah (average price)	$40 618.00
Maintenance	
10 minutes	$ 5 000.00
Crew	
Pilots (2)	$ 346.00
Flight Attendant (1)	54.00
Food & Beverage	
Peanuts	$ 12.50
Beverage	15.00
Equipment Depreciation	
Per flight cost	$ 295.00

The total operating costs for a 1233 meter flight based on an average fuel cost of $90 per mah of fuel is $46,340.50. The cost of the crew was based on an average annual salary of $75,000 for each pilot and $27,500 for the flight attendant. Estimating that each flight would take 190 minutes real world time (150 min for flight, 10 min for maintenance, and 30 min for ground handling), it was assumed that each plane would only complete four 1233 meter flights per day. This came out to be 1040 flights per year, allowing time for routine maintenance and other unexpected down time. The cost per flight for each crew member was then calculated taking into account that a pilot may only work a maximum of 960 hours per year. This means that the Nood Rider 821™ requires approximately 4.33 pilots annually for operation. Based on the above yearly salaries and the crew requirements, we predicted the total crew cost to be $400 per flight. The food and beverage costs were based on $0.25 per bag of peanuts and $0.30 per beverage. The

equipment cost is based on replacement of the aircraft on an annual basis. Therefore, this cost is arrived at by dividing the total unit cost by the total number of flights per lifetime, 1040. The relative magnitudes of the individual costs can be visualized in Figure 8.3.

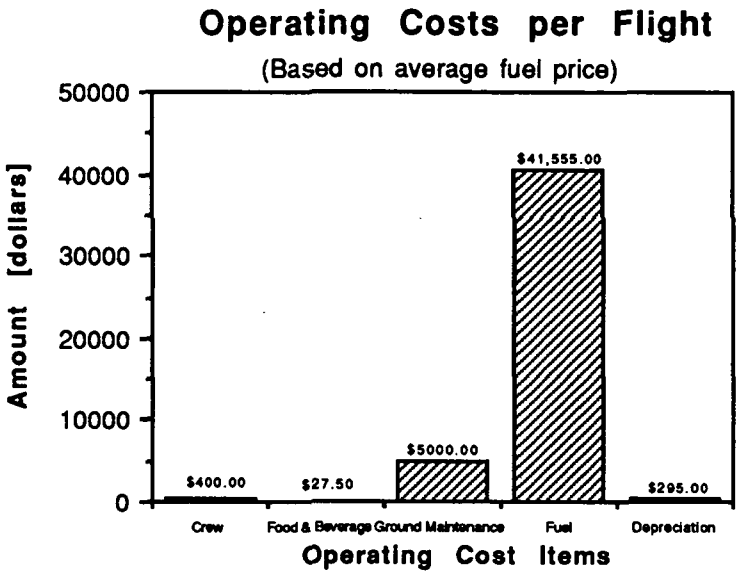

Figure 8.3

8.3 Revenue

The third aspect looked at was ticket price. The number of passengers, operating cost, and ticket price were varied. The operating cost varied due to the range of fuel prices given. The final ticket price was chosen based on the average fuel price. The ticket price was set simply by plotting five different ticket prices versus the number of paying passengers. Superimposed on the plot are three operating costs (O. C.) corresponding to the different fuel prices. Deciding the ticket price was simply done by checking where the revenue from passengers intersects the operating cost line. Where the lines meet, revenue equals cost. When the revenue line is above the operating cost line, the difference equals the operating profit. This can be easily seen in Figure 8.4. The ticket price chosen from this plot was $12.00 per 50 feet (15.24 m). This yields a total revenue of $53,540 per flight.

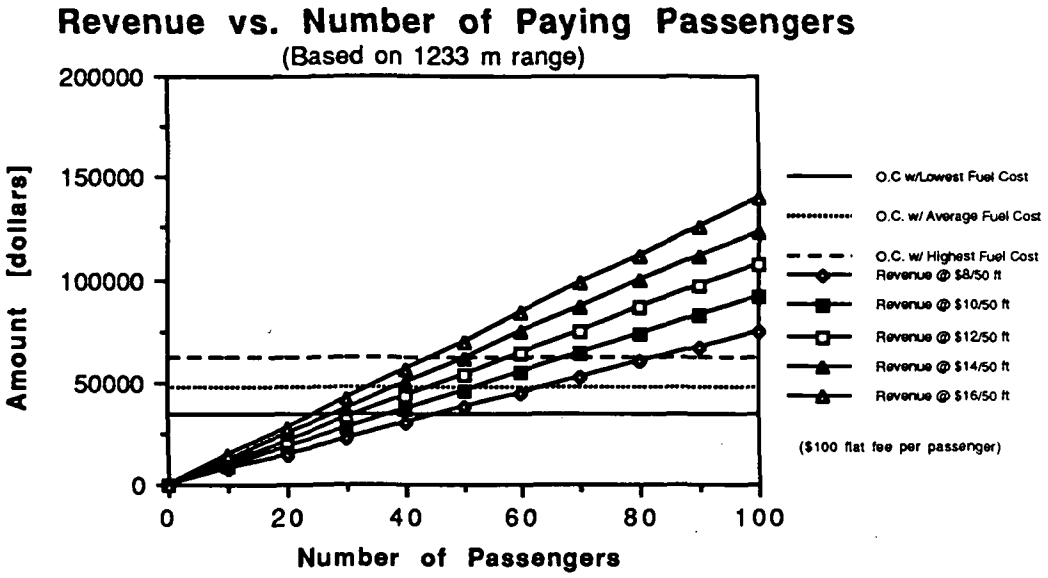

Figure 8.4

8.4 Profit

The total operating profit per flight yielded by the Nood Rider 821™ is determined by subtracting the operating cost per flight from the revenue earned per flight. This yields an operating profit per flight of $7,200. Each aircraft would earn $28,800 per day or $7,488,000 per year. However, it must be pointed out that this is under ideal operation. The passenger load will not always be 100%, and fuel prices will fluctuate. Assuming that only 70% of the operating profit is actually realized, each aircraft will earn $5,241,600 per year. This profit will then be used to maintain current aircraft and pay for new aircraft, as well as cover the expenses incurred by the ground crews and other airline personnel.

9. TECHNICAL DEMONSTRATOR

9.1 Construction

In an attempt to test the airplane which we had designed, we set about constructing a technical demonstrator. The purpose of the technical demonstrator was to test the specific aspects of the airplane. These would include the basics such as the wings, fuselage, empennage, landing gear and propulsion system, but also the parts which make the Nood Rider™ different from most other aircraft, the twin motors, the hinged wings, and the cylindrical fuselage.

One of the toughest parts in constructing the airplane was the fashioning of the fuselage. Because of the fact that it was cylindrical, we decided to cut out bulkheads and run longerons between them. Of course, our fuselage narrows at both the front and the back of the plane so we were forced to cut each bulkhead individually. In addition, because of the high, one-piece wing which was used, the bulkheads in that area had to be cut to support the wing. Finally, we used .158 cm balsa as longerons, both for the rigidity that they gave to the structure and for their use in keeping the fuselage's shape.

The only difficulty involved with the construction of the wing was the hinged sections on the wingtips. We eventually came up with a hinge which would allow us to pivot the wingtips up and above the wings to allow for easy maneuvering into the 1.52 meter gates. Besides the wingtips, we also experienced a slight problem with wing warping, which was corrected by manipulating the Monokote™ coating.

The dual motor concept was destined to give us problems in its realization, but no problems have really appeared. The motors are mounted on the edge of a 35.56 cm aluminum sheet, 5.08 cm in width by .238 cm thick, using two hose clamps per side. These should demonstrate one of the important features of the Nood Rider™, its easily serviceable motors. Because of availability problems we were forced to use Sanyo 1100 Mah batteries in place of the Panasonic 900 Mah batteries that were in the specifications, but we feel that the additional weight will not have a major adverse effect on the performance. Finally, even though we had hoped to have the motors spinning in opposite directions to counterbalance any moment, we were unable to accomplish this on the technical demonstrator.

The control surfaces did not give us any problems and we were able to mount the servo-mechanisms in such a manner that the surfaces could be easily actuated. We placed the ailerons inboard of the wingtips so that we would not need to send the control rods through the hinged areas. This required a little larger surface because of the shorter moment arm but that was not a problem.

In order to deal with the requirement of a timed battery exchange, we made half of the front section removeable as an access panel. The batteries, servos and controllers were placed on balsa sleds to keep them from sliding around during flight, and also to make them easily accessible in case the need arises to fix one of them.

Finally, we placed the main landing gear just forward of the quarter chord of the wing, in order that the center of gravity should be behind it. This will keep the plane stable during ground roll activities.

The total construction time for the Nood Rider 821™ was 125 hours. We feel that, while being greater than anticipated, this figure will decrease with each plane built.

9.2 Weight Comparison

The weights for the technical demonstrator can be broken down as follows:

ITEM	MASS
Propulsion system: 2 motors, batteries, controller	1107 grams
Fuselage: 2 servos, control rods, engine mounts landing gear	481 grams
Wing: 1 servo, control rod	419 grams
Horizontal tail:	57 grams
Vertical tail:	21 grams
Receiver:	30 grams

Figure 9.1

this yields a total mass of 2.115 kg, which is less than the 2.24 kg expected. We figure that the difference is probably due to the balsa being a little lighter than expected, and the fact that we removed circles of wood from non-loadbearing members wherever possible.

APPENDIX A

A.1 Drag Breakdown

The drag of the Nood Rider 821 was estimated using the drag breakdown method. Using this method the contribution of each individual part of the aircraft was summed after being referenced to the area of the main wing. The total contribution to the total skin friction drag was then calculated using:

$$C_f = S_{ref} \sum C_{do} \frac{S}{S_{ref}}$$

The following is a breakdown of the contribution of the various parts of the aircraft to the overall skin friction drive.

Wetted Areas

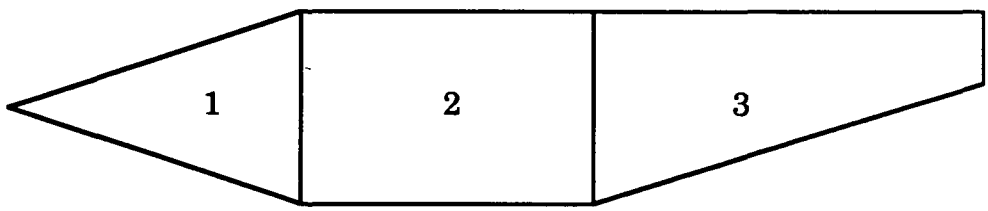

Fuselage
Figure A.1

Wetted Areas in m^2

Fuselage
1. .032
2. .114
3. .182

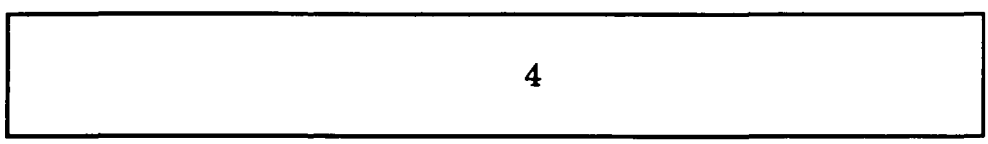

Wing
Figure A.2

Wing
4. 1.047

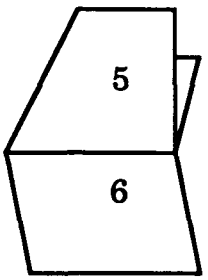

Tail Surfaces
Figure A.3

Tail Surfaces
5. .039
6. .155

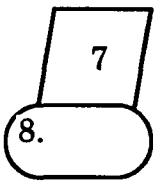

Pylons and Cowling
Figure A.4

Pylons & Cowling
7. .026
8. .024

Total Wetted Area= 1.638 m^2
Cf(skin friction) =.0055*1.638/.5427=.0166

The factor of .0055 was selected based skin friction coefficients of other model aircraft.

Next the drag due to appendage pressure drag was calculated. The drag due to the landing gear and engine nacelles was estimated using Hoerner. For the landing gear configuration on the Nood Rider , the contribution of the gear was estimated to be Cd=.55 S/S_{ref}=.00131. For the engine covering and intake drag, the contribution was estimated to be .008 for each engine, this again from Hoerner. Finally, drag due to component interference was estimated to add an addition 15% to the overall drag. In all, the overall C_{do} of the Nood Rider was estimated to be .0298.

APPENDIX B

B.1 Fuselage Structure

Fuselage Stress Analysis:

$$\sigma_{xx} = -(E/E_1)\, M_z y / I_{zz} + -(E/E_1)\, M_y z / I_{yy}$$

$I_{yy} = I_{zz} = 2*(1/12\, bh^3) + 2*(1/12 hb^3) + bh(D/2 - t/2)^2$

Mz = 2.67 N.m

My = 1.5 N.m

y = z = 19.05 cm

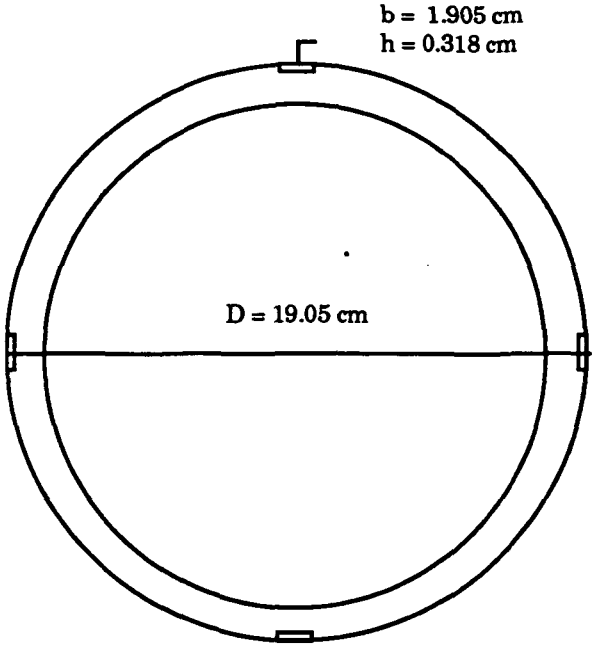

B.2 Wing Structure

Quarter Chord Spar - Stress Analysis Calculations:

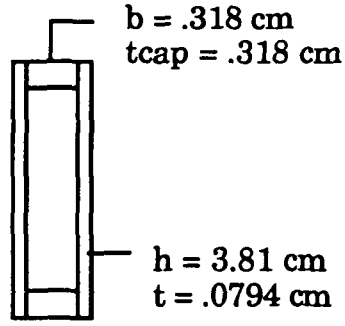

$I_{yy} = 2*\{E/E_1(1/12 tcap*b^3) + E/E_1((1/12\ ht^3) + ht*(b/2 + t/2)^2\}$

$I_{zz} = 2*\{E/E_1((1/12\ b*tcap^3) + b*tcap*((h-tcap)/2)^2 + E/E_1(1/12\ th^3)\}$

$M_y = 11.4$ N.m

$M_z = .87$ N.m

y = 1.905 cm
z = .2 cm

B.3 Empennage Structure

Empennage Stress Analysis:

$\sigma_{xx} = M_z\ y / I_{zz}$

Horizontal Tail:

Spar cross-section:

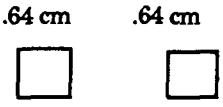

$I_{zz} = 2*(1/12\ bh^3)$

y = .32 cm

Mz = .15 N.m

$\sigma_{xx} = 1.8 \times 10^6$ N/m^2

Vertical Tail:

Structural Cross-section:

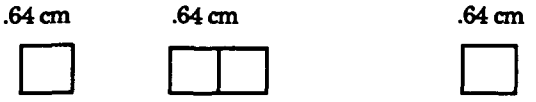

$I_{zz} = 2*(1/12\ bh^3) + 1/12*(2b)*h$

$y = .32$ cm

$Mz = .366$ N.m

$\sigma_{xx} = 2.144 \times 10^6$ N/m^2

APPENDIX C

C.1 Takeoff Thrust Calculations

In ground roll, the basic equation of motion is:

$$T = D + \mu(W - L) + ma \qquad C.1$$

where T is the thrust, D is the drag, μ is the coefficient of rolling friction, W is the weight, L is the lift, m is the mass, and a is the acceleration. Two of these quantities can be broken down further. The drag becomes:

$$D = \frac{1}{2}\rho V_\infty^2 \left(C_{D_0} + \frac{(C_{L\alpha}\,\alpha)^2}{\pi\, AR\, e}\,\phi\right) \qquad C.2$$

where ρ is the density of air, V_∞ is the velocity of the flow, C_{D_0} is the form drag coefficient, $C_{L\alpha}$ is the finite wing lift curve slope, α is the angle of attack, AR is the aspect ratio of the wing, e is the oswald efficiency factor, and ϕ is an empirical factor determined from the equation:

$$\phi = \frac{(5h/b)^2}{1+(5h/b)^2} \qquad C.3$$

where h is the height of the wings above the ground and b is the wingspan. In a similar manner, $C_{L\alpha}$ is determined from the infinite wing lift curve slope a_0 such that:

$$C_{L\alpha} = \frac{a_0}{1+\frac{a_0\phi}{\pi\, ARe}} \qquad C.4$$

At this point we could break down the second quantity, the lift, but a careful look at the value of the lift just prior to takeoff shows that it will be at least equal to, if not greater than, the weight at that point. Also, knowing that a common value for μ on pavement is 0.02, we can deduce that the contribution of this term will be nearly zero anyway.

We have, therefore, reduced our equation for thrust required at takeoff to:

$$T = D + ma \qquad C.5$$

which appears to be a much more manageable size for us to deal with.

We know that the acceleration is the rate of change of velocity with time $\frac{dv}{dt}$, but it can also be expressed as $\overline{V}\frac{dv}{dx}$, where $\overline{V}$ is the average velocity during takeoff. Knowing that the initial velocity is zero, we can calculate takeoff velocity, V_{to}, from:

$$V_{to} = 1.2\sqrt{\frac{2W}{\rho\, C_{Lmax} S}} \qquad \text{C.6}$$

where C_{Lmax} is the maximum lift coefficient attainable, S is the planform area, and the other variables are as defined above, such that $\overline{V}$ becomes $\frac{V_{to}}{2}$.

C.2 Cruise Thrust Calculations

At cruise, thrust is equal to drag. Therefore, since we are no longer in ground effect,

$$T = \frac{1}{2}\rho\, V_\infty^2 \left(C_{Do} + \frac{(C_{L\alpha}\,\alpha)^2}{\pi\, AR\, e}\right) \qquad \text{C.7}$$

where each of the values is as it was before.

C.3 Output from Takeoff Performance Code

```
GROUPe
4.05            ! WEIGHT IN LBS
5.83            ! WING REF AREA IN FT2
.002378               ! AIR DENSITY SLUG/FT3
1.              ! CL AT TAKEOFF ATTITUDE
.076            ! CD AT TAKEOFF ATTITUDE
1.15            ! CLMAX -
75.             ! LIMIT ON TAKEOFF DIST FT
.1              ! FRICTION COEFFICIENT
.667            ! PROP DIAMETER IN FT
9.6             ! BATTERY VOLTAGE
.615            ! KT IN in-oz/amp
.000467               ! KV IN volts/rpm
.055            ! armature resistance
.056            ! battery resistance
20.             ! FUSE AMPS - MAX DRAW
2.2             ! gear ratio
.05             ! INTEGRATION TIME INCREMENT
40.             ! limit on take-off time (SEC)
9               ! number of prop data points
0       .012    .009
.23     .115    .031
.3      .097    .032
.37     .077    .031
.44     .055    .026
.48     .044    .023
.51     .033    .019
.55     .022    .015
10      0.      -100.
```

C.4 Thrust, Power, Voltage, and Current Calculations

mass (kg)	span (m)	chord (m)	wing height (m)	dto (m)	alpha (degrees)	S (m2)
2.22	2.13	0.254	0.254	15	4.5	0.5
ao (/rad)	CDo	CLmax	e	rho (kg/m3)	g (m/s2)	mur
5.58	0.0298	1.14	0.869	1.225	9.8	0.
AR	phi	cla cruise (/rad)	cla to (/rad)	Vto (m/s)	drag lo (N)	cruise drag (N)
8.386	0.262	4.486	5.245	9.107	2.25	2.8
mus	alpha L=0.0	alpha i				
0.1	4	3.75				
accel (m2/s)	thrust at lo (N)	static thrust (N)	cruise thrust (N)	PR at lo (W)	PR at cruise (W)	
2.764	8.387	6.359	2.816	76.373	28.161	
	V = 10 m/s	cruise	V= Vto	takeoff	thrust avail	at cruise
advance ratio	n @ 8 in	n @ 9in	n @ 8 in	n @ 9 in	8 in	9 in
takeoff						
0.29	169.698615	150.843214	154.538587	137.367633	4.48703963	5.526017
0.291	169.115459	150.324852	154.007527	136.895579	4.44697538	5.470085
0.292	168.536296	149.810041	153.480104	136.426759	4.40733617	5.414768
0.293	167.961087	149.298744	152.956281	135.961138	4.36811612	5.360057
0.294	167.389791	148.790925	152.436021	135.498686	4.32930943	5.305944
0.295	166.822368	148.286549	151.919289	135.039368	4.29091043	5.252420
0.296	166.258778	147.785581	151.406048	134.583154	4.25291352	5.199477
0.297	165.698985	147.287986	150.896264	134.130012	4.2153132	5.147107
cruise						
0.42	117.172853	104.153647	106.705215	94.8490799	1.4889077	1.42701
0.421	116.894533	103.906252	106.451758	94.6237852	1.47630998	1.410352
0.422	116.617532	103.660028	106.199503	94.3995582	1.46380639	1.393822
0.423	116.34184	103.414969	105.94844	94.1763914	1.45139601	1.377422
0.424	116.067449	103.171066	105.698562	93.9542773	1.43907795	1.361151
0.425	115.794349	102.92831	105.449859	93.7332084	1.42685131	1.345009
0.426	115.522532	102.686695	105.202325	93.5131774	1.41471522	1.32899
0.427	115.251987	102.446211	104.955949	93.294177	1.40266881	1.313103
0.428	114.982707	102.20685	104.710725	93.0761999	1.39071121	1.297337

power avail	at cruise	thrust avail	at takeoff	power avail	at takeoff	efficiency
8 in	9 in	8 in	9 in	8 in	9 in	8 in
54.2128169	69.7050756	3.72115006	4.58278525	40.9428331	52.6429623	0.648264
53.6821054	68.987573	3.68792434	4.53640059	40.5420269	52.1010869	0.648862
53.1581184	68.278581	3.65505112	4.49052573	40.1462992	51.5656389	0.649455
52.6407399	67.5779723	3.62252551	4.44515351	39.7555624	51.0365223	0.650043
52.1298567	66.8856222	3.59034271	4.40027685	39.3697311	50.5136427	0.65062
51.6253579	66.2014078	3.55849801	4.35588883	38.9887213	49.9969074	0.651207
51.1271348	65.5252089	3.52698676	4.31198263	38.6124512	49.4862256	0.651781
50.6350812	64.8569072	3.49580441	4.26855156	38.2408404	48.981508	0.652352
17.2101087	19.2416435	1.23476712	1.183439	12.9974911	14.5317555	0.696114
17.0639893	19.0482848	1.22431969	1.1696207	12.8871382	14.3857263	0.696254
16.9190165	18.8565934	1.21395033	1.15591178	12.7776513	14.2409563	0.696390
16.7751785	18.6665517	1.20365827	1.14231117	12.6690213	14.0974322	0.696521
16.6324634	18.4781425	1.19344277	1.12881779	12.5612394	13.955141	0.696648
16.4908596	18.2913486	1.18330309	1.11543057	12.4542968	13.8140697	0.696770
16.3503555	18.1061534	1.1732385	1.10214847	12.3481847	13.6742058	0.696887
16.2109398	17.9225401	1.16324827	1.08897046	12.2428946	13.5355366	0.697000
16.0726015	17.7404922	1.15333171	1.07589551	12.1384181	13.3980496	0.697108
	motor Q at TO		motor Q at cruise		current draw at	cruise
9 in	8 in (in-oz)	9 in (in oz)	8 in (in-oz)	9 in (in-oz)	8 in	9 in
0.63977581	3.44959031	4.84280164	3.78799049	5.31787398	7.97679747	10.46093
0.63981574	3.42741745	4.81001532	3.7636425	5.28187137	7.93726253	10.40248
0.6398506	3.40542643	4.77747529	3.73949419	5.24613921	7.89805181	10.34446
0.63988045	3.38361481	4.74517831	3.71554289	5.21067393	7.85916099	10.28687
0.63990531	3.36198022	4.71312121	3.69178597	5.17547207	7.8205858	10.22971
0.63992524	3.34052031	4.68130089	3.66822087	5.14053023	7.78232207	10.1729
0.63994026	3.31923278	4.64971432	3.64484506	5.10584505	7.7443657	10.11665
0.63995042	3.29811536	4.61835852	3.62165605	5.0714133	7.70671265	10.06074
0.59151217	1.54382525	1.95897312	1.69527243	2.15114575	4.57875561	5.318977
0.59042049	1.53409842	1.94429746	1.68459141	2.13503043	4.56141236	5.292810
0.58930973	1.52442119	1.92970322	1.67396486	2.11900452	4.54415754	5.266788
0.58817962	1.5147932	1.91518976	1.66339238	2.10306731	4.52699051	5.240910
0.58702989	1.50521408	1.90075647	1.65287356	2.08721813	4.50991064	5.215175
0.58586028	1.49568348	1.88640269	1.64240803	2.07145627	4.49291727	5.189582
0.58467052	1.48620105	1.87212781	1.63199538	2.05578104	4.47600978	5.16412
0.58346034	1.47676643	1.85793119	1.62163523	2.04019175	4.45918753	5.138816
0.58222946	1.46737927	1.84381218	1.61132721	2.02468768	4.44244992	5.113642

current draw	at TO	battery	voltage cruise	battery	voltage TO
8 in	9 in	8 in	9 in	8 in	9 in
7.42732164	9.68954249	11.3301818	10.2224934	10.8203017	9.3272113
7.39131856	9.63630585	11.2900937	10.186031	10.7829917	9.29400627
7.35561073	9.58346912	11.2502855	10.1498242	10.7459379	9.26103402
7.32019422	9.53102703	11.2107543	10.1138704	10.7091375	9.22829207
7.28506515	9.47897445	11.1714972	10.0781667	10.6725881	9.19577797
7.25021971	9.42730635	11.1325112	10.0427105	10.636287	9.16348931
7.21565417	9.37601779	11.0937934	10.0074993	10.6002317	9.1314237
7.18136485	9.32510395	11.0553412	9.97253049	10.5644198	9.09957881
4.3328439	5.00693845	7.73571083	6.95619468	7.46153458	6.35270739
4.31705001	4.98310892	7.71673099	6.93896024	7.44374464	6.33701259
4.30133665	4.95941159	7.69784173	6.92180817	7.42603909	6.3213928
4.28570324	4.93584543	7.6790424	6.90473788	7.40841731	6.30584749
4.27014919	4.91240942	7.66033236	6.88774879	7.39087873	6.29037612
4.25467393	4.88910255	7.64171098	6.87084032	7.37342275	6.27497817
4.23927687	4.86592377	7.62317764	6.85401191	7.35604879	6.25965312
4.22395744	4.84287206	7.60473172	6.83726298	7.33875628	6.24440046
4.20871508	4.81994638	7.58637259	6.82059298	7.32154463	6.22921968

APPENDIX D

D.1 Stability and Control Analysis Computer Code

```
5 REM PROGRAM TO DETERMINE STABILITY OF NOOD RIDER

10 LET CDO=.0298
20 LET E=.87
30 LET W=9.81*1.85
40 LET S=.542
50 LET AR=8.4
60 LET C=.254
70 LET CLALPH=4.487
80 LET CLAW=4.487
90 LET WCHORD=.254
100 LET Q=61.25
110 LET ST=.0619
120 LET LT=.681
130 LET LV=.68
140 LET U=10
150 LET MASS=1.85
160 LET SV=.02322
170 LET CDU=0
180 LET XCG=.2921
190 LET CLAT=3.8
200 LET DEDA=.3225
210 LET DCLTDE=3.8*.35
220 LET CLO=.4

1000 LET VH=ST*LT/S/WCHORD
1010 LET VT=SV*LV/S/WCHORD
1020  LET CDU=.7225/3.14/E/AR:LET CLU=.4
1500 LET CXU=-(CDU+2*CDO)+CTU
2000 LET CXAL=CLO-(2*CLO/3.14159/E)
3000 LET CZU=-(M^2/(1/M^2))*CLO-2*CLO
4000 LET CZAL=-CLALPH+CLO
5000 LET CZALD=-2*CLAT*VH*DEDA
6000 LET CZQ=-2*CLAT*VH
7000 LET CZDE=-ST/S*DCLTDE
8000 LET CMU=0
8010 LET XU=-(2*CDO)*Q*S/MASS/U
8020 LET ZU=-(2*CLO)*Q*S/MASS/U
9000 PRINT "ZU="ZU
10000 LET CMALD=-2*CLAT*VH*LT/2*DEDA
11000 LET CMQ=-2*CLAT*VH*LT/C
12000 LET CMDE=VH*DCLTDE
20000 LET ZAL=(-1)*(CLALPH+CDO)*Q*S/MASS
20010 LET CMAL=CLAW*(-.04115)-VH*CLAT*(1-DEDA)
20021 LET IY=7.34
20025  LET WNP=(-1*ZU*9.81/U)^.5
```

```
20030 PRINT" WNP=" WNP
20035 LET SIGP=XU/2/WNP*(-1)
20040 PRINT " SIGP=" SIGP
20050 LET MQ=CMQ*C*Q*S*C/2/U/IY
20060 LET MALD=CMALD*C*Q*S/U/IY

20075 LET MAL=CMAL*Q*S*C*IY
20078 PRINT "ZAL="ZAL:PRINT "MQ="MQ:PRINT "MAL="MAL
20079
20080 LET WNSP=(((ZAL*MQ)/U)-MAL)^.5


20090 LET SIGSP= -1*((MQ+MALD+(ZAL/U))/2/WNSP)
20100 PRINT "WNSP="WNSP
20110 PRINT "SIGSP="SIGSP
```